Universiteit
Leiden
The Netherlands

# Biomechanical studies on type B aortic dissection

Veger, H.T.C.

**Citation**
Veger, H. T. C. (2022, March 24). *Biomechanical studies on type B aortic dissection*. Retrieved from https://hdl.handle.net/1887/3280049

| | |
|---|---|
| Version: | Publisher's Version |
| License: | Licence agreement concerning inclusion of doctoral thesis in the Institutional Repository of the University of Leiden |
| Downloaded from: | https://hdl.handle.net/1887/3280049 |

**Note:** To cite this publication please use the final published version (if applicable).

# Biomechanical Studies on Type B Aortic Dissection

**Hugo Thomas Christian Veger**

ISBN 978-94-6361-607-2

Layout and printed by Optima Grafische Communicatie, Rotterdam, the Netherlands

© 2022 Hugo Veger
All rights reserved. No part of this thesis may be reproduced, stored or transmitted in any way or by any means without the prior permission of the author, or when applicable, of the publishers of the scientific papers.

# Biomechanical Studies on Type B Aortic Dissection

**Proefschrift**

ter verkrijging van
de graad van doctor aan de Universiteit Leiden,
op gezag van rector magnificus prof.dr.ir. H. Bijl,
volgens besluit van het college voor promoties
te verdedigen op

donderdag 24 maart 2022
klokke 13:45 uur

door

**Hugo Thomas Christian Veger**
geboren te Dronten
in 1982

**Promotor**
prof. dr. J.F. Hamming

**Copromotor**
dr. R.G.S. van Eps

**Review committee**
prof. dr. P.H.A. Quax
Department of Experimental Vascular Medicine
Leiden University Medical Center

dr. ir. J.J.M. Westenberg
Department of Radiology
Leiden University Medical Center

prof. dr. M.D. Ackermann
Department of Physics
University of Twente

dr. A. Schepers
Department of Vascular Surgery
Leiden University Medical Center

prof. dr. J.A. van Herwaarden
Department of Vascular Surgery
University Medical Center Utrecht

## CONTENTS


| | | |
|---|---|---|
| Chapter 1. | Introduction to acute aortic type B dissection.<br>Aims and outline of the thesis. | 7 |
| Chapter 2. | The role of branch vessels in aortic type B dissection. An in-vitro study. | 23 |
| Chapter 3. | The influence of aortic wall compliance on false lumen expansion in aortic dissection. An in-vitro study. | 37 |
| Chapter 4. | Wall shear stress assessment of the false lumen in acute type B Aortic dissection visualized by four-dimensional flow magnetic resonance imaging (4D flow MRI). An ex-vivo study. | 47 |
| Chapter 5. | Where to fenestrate in type B aortic dissection? An ex-vivo study. | 61 |
| Chapter 6. | General discussion | 71 |
| Chapter 7. | Summary<br>Samenvatting in het Nederlands | 81 |
| Chapter 8. | List of Abbreviations | 89 |
| | Acknowledgements (Dankwoord) | 90 |
| | List of Publications | 91 |
| | Curriculum Vitae | 93 |

# Introduction to Acute Aortic Type B Dissection

Adapted from; Understanding Acute Aortic Type B Dissection:
Are There New Horizons In Patient Selection?

H.T.C. Veger
J.F. Hamming
M.J.T. Visser

Reviews in Vascular Medicine. 2013

## HISTORY

The dissection process of blood vessels was first described more than three hundred years ago by Sennertus. However the first detailed descriptions of the clinical entity was published by the British physician named Nicholls in 1760. [1] In 1802 Maunoir described the penetration of blood through the media of a diseased aorta. At the end of the 19th century the first correct ante-mortem diagnosis of aortic dissection was made by Swaine. It took almost half a century before the first surgical intervention with an aortic fenestration procedure was attempted to treat malperfusion syndrome. The first primary open surgical repair of an acute aortic dissection was performed by De Bakey and Cooley in 1954. [2] The first reports of endovascular repair of acute aortic dissection with stent graft technology were at the end of the 20th century. [3]

## PATHOFYSIOLOGY

Aortic dissection (AD) begins with an intimal tear which allows blood to enter and split the medial layers. Intimal disease, such as that associated with atherosclerosis, is not a prerequisite, although underlying medial disease due to both elastic fiber and smooth muscle cell degeneration is the rule. [4]

The most frequent site of entry in the descending thoracic aorta is just beyond the insertion of the ligamentum arteriosum, where the relatively mobile arch becomes anchored to the thoracic cage. Aortic dissection results in a false and true lumen. The false lumen having pressures greater than or equal to those in the true lumen. Expansion of the false lumen occurs due to its thin outer wall, which contains only about one-third of the elastin of the total vascular wall. The elastin-poor outer wall of the false lumen then dilates more than the elastin-rich nondissected inner wall to generate the wall tension required to balance a given blood pressure. [5] Dilatation of the false lumen is multi-factorial and depends on the (intra-luminal) blood pressure, residual wall thickness (depth of dissection plane in the media; wall shear stress), percentage of the wall circumference involved in the dissection. The dissection can evolve in either an antegrade or retrograde direction. Because of pressure differences, the false lumen may compress or obstruct the true lumen. [6] In general, after dissection several sequelae can occur. Acute dissection may be complicated by loss of blood supply to a vital organ because of branch arterial obstruction with either dynamic or static mechanisms. [6] In static obstruction, the dissection flap enters the branch vessel with absent or inadequate distal re-entry and causes ischemia by reducing the true lumen diameter. In contrast, the dissection flap in dynamic obstruction intermittently prolapses across the orifice of the branch vessel during the cardiac cycle, and this subsequently results in end-organ ischemia. [6] The false lumen may remain patent, thrombose, recommunicate with the true lumen through fenestrations, or rupture.

## AETIOLOGY

Aortic dissection results from an interaction between abnormal hemodynamic circumstances and / or abnormal morphological characteristics of the aortic wall.

The two causes of abnormal hemodynamic factors are hypertension - found in at least two-thirds of all cases - and aortic coarctation. Causes of abnormal morphological characteristics of the aortic wall can be due to atherosclerosis, connective tissue disorders, iatrogenic factors or trauma (Tabel I). [6]

**Tabel I.** Conditions contributing to abnormal morphological characteristics of the aortic wall

| | | |
|---|---|---|
| Atherosclerotic Risk factors | | Hypertension |
| | | Dyslipidemia |
| | | Smoking |
| | | Cocaine |
| Connective tissue disorders | Congenital | Bicuspid aortic valve |
| | | Cystic medial necrosis |
| | | Turner's syndrome |
| | | Marfan syndrome |
| | | Ehlers-Danlos syndrome |
| | | Loeys-Dietz syndrome |
| | Hereditary | Familial thoracic aortic aneurysm |
| | Acquired | Giant cell arteritis |
| | | Takayasu's arteritis |
| | | Syphilitic aortitis |
| | | Behcet disease |
| Iatrogenic | | Aortic catheterization |
| | | Aortic (valve) surgery |
| | | TEVAR |
| Trauma | | Deceleration injuries |

Cocaine serves as both a predisposing factor to aortic dissection due to its effect on aortic connective tissue and as a precipitating factor due to its propensity to produce abrupt and severe hypertension. [7]

Connective tissue disorders can be congenital, hereditary or acquired. Congenital causes includes bicuspid aortic valve and is associated with aortic aneurysm and dissection. This suggests the possibility that a bicuspid valve is an identifiable manifestation of a systemic connective tissue disorder. [8] In cystic medial necrosis there is a degenerative breakdown of collagen, elastin and smooth muscle caused by aging contributing to weakening of the wall of the artery. Turner's syndrome is associated with high blood pressure and aortic dilatation. [9] Structural weakness of the aortic wall is associated with multiple connective tissue disorders such as Marfan syndrome, Ehlers-Danlos and Loeys-Dietz syndrome. [6]

Acquired disorders include inflammatory diseases, which can destroy the medial layers of the aortic wall and lead to weakening, expansion, and dissection of the aortic wall. [9] Autoimmune processes may affect vasa vasorum and promote nutrient deficiency of aortic wall layers. [9] Iatrogenic aorta dissections can result from aortic (valve) surgery, aortic catheterization or after Thoracic EndoVascular Aortic Repair (TEVAR). Rare but not uncommon is aorta dissection after high deceleration trauma.

## INCIDENCE OF AORTA DISSECTION

Aortic dissection is the most frequently diagnosed lethal condition of the aorta and occurs nearly three times as frequent as rupture of abdominal aortic aneurysm. [10] The overall incidence of aortic dissection has been estimated to 2.9 to 3.5 cases per 100 000 person-years. [6] The mean age at presentation is reported at around 60 years. [11] Males are more frequently affected than females, the rate is considered between 2:1 and 5:1. [9] Women may be affected less frequently, but have worse outcome as a result of atypical symptoms and delayed diagnosis. [9]

An important risk factor is a positive family history of thoracic aortic diseases. Acute TBAD has a prevalence of 13- 22% in patients who have a first degree relative with a history of descending thoracic aneurysm or AD. 6

## CLASSIFICATION

### Anatomical

The Stanford classification system of AD, described in 1970, has come to be the most widely used in the literature. Type A affects the ascending aorta proximal of the brachiocephalic artery, type B distally (Figure 1.). The most frequent site of entry in the descending thoracic aorta is just beyond the insertion of the ligamentum arteriosum, where the relatively mobile arch becomes anchored to the thoracic cage.

Recently a new anatomical classification system was introduced by the Society for Vascular Surgery/Society of Thoracic Surgeons (SVS/STS). This is based on the location of the entry tear and the proximal and distal extent and redefines nomenclature associated with Type B Aortic Dissection (TBAD) (Figure 2.). [12]

This new classification provides a clear framework of language that will allow more granular discussions and reporting of aortic dissection in the future. [12]

### Complications

Complicated TBAD (cTBAD) is associated with rupture, mal-perfusion syndrome, refractory pain, rapid aortic expansion at onset or during hospital stay and failure of medical management

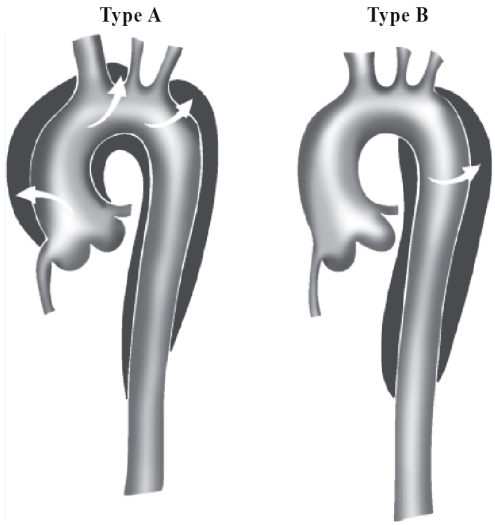


**Figure 1.** Stanford classification system of aortic dissection

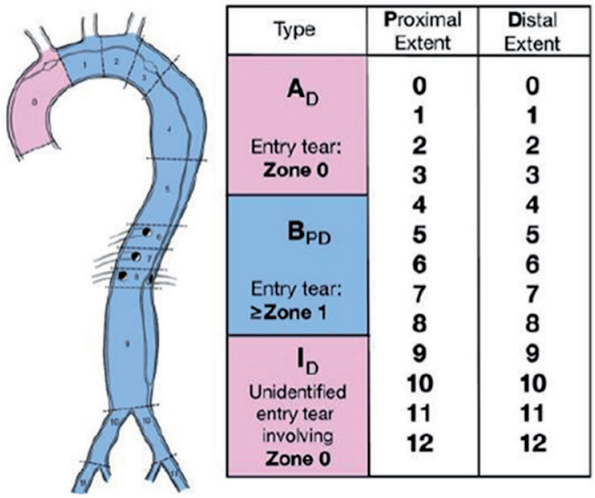

| Type | Proximal Extent | Distal Extent |
|---|---|---|
| $A_D$ Entry tear: Zone 0 | 0 | 0 |
| | 1 | 1 |
| | 2 | 2 |
| | 3 | 3 |
| $B_{PD}$ Entry tear: ≥Zone 1 | 4 | 4 |
| | 5 | 5 |
| | 6 | 6 |
| | 7 | 7 |
| | 8 | 8 |
| $I_D$ Unidentified entry tear involving Zone 0 | 9 | 9 |
| | 10 | 10 |
| | 11 | 11 |
| | 12 | 12 |

**Figure 2.** Society for Vascular Surgery (SVS) and Society of Thoracic Surgeons (STS) reporting standards for type B aortic dissections. [12]

(see paragraph Treatment). Uncomplicated TBAD (uTBAD) occurs without the aforementioned complications.

## Time of onset

A subdivision in onset of uTBAD is "acute" and should refer to <2 weeks, "subacute" from 2 to 6 weeks, and "chronic">6 weeks from symptom onset.

## CLINICAL PRESENTATION

Acute AD is clinically suspected at initial evaluation in fewer than half of patients ultimately diagnosed with the disease. [9] Acute aortic dissection is frequently confused with acute coronary syndrome, resulting in delayed diagnosis and inappropriate treatment with antiplatelet, antithrombin, and fibrinolytic therapies. On the other hand a variety of symptoms can initially suggest acute aortic dissection but ultimately prove to represent other conditions. The stimulated sensory fibers in acute aortic dissection may share the common spinal segments with those arising from the heart, pericardium, pleura, and esophagus. [13]

The majority of patients with dissections have a previously documented history of hypertension (sensitivity 64%). [13] Most patients with acute aortic dissection present with pain (sensitivity 90%) of severe intensity (sensitivity 90%) with sudden onset (sensitivity 84%). [13.] The presence of a tearing and ripping pain sensation has a specificity around 95%. [14] Clinical findings for thoracic AD during physical examination are present in less than half of all cases. [14] The sensitivity of a clinical finding suggesting a dissection is disappointing with a reported sensitivity of only 31% in case of pulse pressure differential between carotid, radial and femoral arteries. [14]

## IMAGING

In the 20$^{th}$ century aortography was used as the best imaging technique for assessing patients with clinically suspected thoracic aortic dissection. Currently, the noninvasive modalities most frequently used to identify aortic dissections are ultrasonography (US), helical computed tomography angiography (CTA) and magnetic resonance angiography (MRA).

US include transthoracic echocardiography (TTE) and transesophageal echocardiography (TEE). The image quality of TTE is adversely affected by obesity, emphysema, mechanical ventilation, chest-wall deformities, or small intercostal spaces resulting in sensitivity between 31%–55% for dissections involving the descending aorta. [5] TEE may be used in the primary care setting to visualize the descending thoracic aorta from the Left Subclavian Artery (LSA) to coeliac artery with sensitivity up to 100%. However TEE in the awake patient can lead to more hypertension introducing more risks. If a patient is intubated for TEE further clinical symptoms are masked by sedation. This has to be balanced in the acute situation. US also have major general shortcomings, the diagnostic accuracy depends largely on the investigator's experience and the images can't be used to plan therapy. [15] This makes US as diagnostic imaging modality for AD not very helpful.

The standard technique for diagnosing and classifying thoracic aortic dissections are contrast-enhanced CTA, 3-dimensional (3D) MRA and 4-dimensional (4D) MRI.

The gold standard for imaging TBAD is Computed Tomography Angiography (CTA). [16] Imaging should include a noncontrast study, followed by an early and late phase contrast study and should examine the part of the body between the thoracic inlet and the common femoral arteries. CTA

has the advantages of shorter acquisition time, wide availability, and high diagnostic accuracy with sensitivity of 100% (CI 95% 96-100) and specificity of 98% (CI 95% 87-99). [17] False-negative CTA results can occur due to inadequate contrast opacification caused by cardiac failure or to the thrombosed lumen being mistaken for an aortic aneurysm with mural thrombus. [5]

Over the last two decades, CTA has become more sophisticated and is more readily available, with an increase in the number of scanners, the use of ECG-gated techniques, and through advances in post-processing software. These advances have resulted in motion free images with higher resolution, reduced scanning times, and better visualisation including three dimensional reconstruction. [18]

A major disadvantage of CTA is the static aspect of images, interpretation of the volume and flow changes in the true and false lumen during cardiac cycle is not possible. Contrast-enhanced 3D MRA has several advantages over CTA, including lack of nonionizing radiation, multiplanar evaluation, "safer" (ie, nonnephrotoxic) contrast material and greater vessel coverage at high resolution with fewer sections. [5] 4D flow MRI can accurately visualize and quantify the functional flow and access hemodynamic information such as as entry tear flow, blood flow patterns in the false and true lumen and Wall Shear Stress (WSS). [19] The WSS expresses the viscous force per unit area applied by the fluid on the wall in a direction at the local interface. [20]

Nevertheless, 3D and 4D MRA has its clinical limitations. It cannot be performed in unstable patients due to longer acquisition time and difficulty in monitoring, and it is also not appropriate for patients with implanted electronic devices or metal implants.

Performing CTA or MRA first for confirming or ruling out thoracic aortic dissection should depend on the availability of each imaging test because time delay increases the mortality rate in untreated patients. [9] However, 3D MRA may prove to be the optimal imaging modality in medically stable patients with aortic dissection. [21]

## TREATMENT

Current treatment modality depends on whether the TBAD is categorized as either uncomplicated or complicated. About one third of the TBADs are complicated. [22] Intractable pain, rapid expansion and/or rupture, and organ and/or lower limb ischemia (malperfusion) are signs of cTBAD. The therapeutic options for cTBAD are endovascular therapy (fenestration and / or TEVAR) and open surgery. Endovascular fenestration can be performed in case of cTBAD with malperfusion syndrome due to dynamic compression. [23] Fenestration of the dissection flap decreases the load and pressure inside the false lumen by increasing communication between the true and false lumen. The concept of TEVAR was propelled by the desire to induce aortic remodeling by means of exclusion of the false lumen and thrombosis of the false lumen and, at the same time, avoiding the risks associated with open surgical intervention. Entry tear coverage with endovascular stent grafting and redirection of thoracic aortic flow entirely through the true lumen have been the hall-

marks of endovascular repair. [24] Creation of a sufficient proximal landing zone by over stenting the left subclavian artery during endovascular stent grafting results in increased risk of perioperative stroke, paraplegia and death. [28] Revascularisation of the LSA offers protection against a composite endpoint of stroke, paraplegia and death. [6 25]

A feared complication after TEVAR is the occurrence of a retrograde dissection. The stress yielded by the endograft seems to play a predominant role in its occurrence. It is important to take this stress-induced injury into account during both design and placement of the endograft. [26] Despite these disadvantages TEVAR provides improved survival in cTBAD with mortality rates of 10% to 20% versus 20% to 30% in open surgery. [6 9] TEVAR is now the treatment of choice for these extremely high-risk and complex patients. [6 9]

uTBAD is diagnosed in the absence of complications and has traditionally been managed medically. Optimal Medical Treatment (OMT) includes observation in an intensive care setting with aggressive blood pressure and heart rate control and close surveillance. [6 9 27] Also sedation and pain reducing management should be included. OMT for all acute uTBAD was derived from early studies conducted several decades ago that demonstrated no survival advantage of surgery over OMT. The goal of OMT is to reduce aortic wall stress and False Lumen (FL) pressurization. In the acute phase, intravenous medications are aimed to control heart rate, blood pressure and reduce the maximum change in left ventricular pressure in early systole (maximum dP/dt). [6 9 11] This result in a decrease aortic wall shear stress. [6 27] Alpha- and betablockers such as labetalol are useful first-line agents. If a potent vasodilator such as sodium nitroprusside is to be used, it is imperative to be certain that the patient is on a beta-blocker with good heart rate control to avoid reflex tachycardia. [3] A significantly decrease is observed of secondary adverse events (aortic expansion, recurrent aortic dissection, aortic rupture and/or need for aortic surgery) by reducing the heart rate below 60 bpm. [6] To achieve a systolic blood pressure of 100 to 120 mm Hg calcium-channel-blockers, nitrates and angiotensin converting enzyme inhibitors can be administered. [27] Approximately 20% of acute uTBAD could progress to a complicated state, with malperfusion syndrome constituting a significant portion of delayed complications. [9] Despite medical management overall in-hospital mortality for uTBAD is around 12%. [11 28] Once complications occur the prognosis declines, with hospital mortality greater than 50%. [29] By evolving medicine in particular improved perioperative management and most important the increased experience of TEVAR the morbidity and mortality from intervention has decreased. This resulted in several studies comparing OMT to OMT+TEVAR in subacute and acute uTBAD.

## Subacute uTBAD

The INSTEAD (Investigation of Stent Grafts in Aortic Dissection) trial randomized 140 patients with subacute uTBAD into cohorts of elective TEVAR with OMT (n = 72) to OMT alone (n = 68). [28] At 2 years, no mortality difference was found for patients that had OMT+TEVAR compared with OMT alone. OMT+TEVAR was associated with improved favorable remodeling, with a FL thrombosis rate of 91.4%, compared with 19.4% in the OMT cohort ($p \leq 0.001$). [28] Extended

follow-up to 5 years in the INSTEAD-XL trial, the OMT+TEVAR patients had improved 5-year aorta-specific mortality (6.9% vs. 19.3%; p = 0.045), as well as greater rates of favorable remodeling (79.2% vs. 10%; p < 0.001). [30] This survival benefit is attributed to the ability of TEVAR to prevent late complications. In the Clinical Practice Guidelines of the European Society for Vascular Surgery (ESVS) patients at risk of further aortic complictions with suitable anatomy for endografting, endovascular repair of uTBADs in the sub-acute phase should be considered in dedicated centres. [6]

### Acute uTBAD

ADSORB is the first and only prospective randomised clinical trial of acute uTBAD. [29] The primary endpoints were false lumen thrombosis, aortic dilatation, and aortic rupture. The original sample size calculation at trial inception in 2002 called for 250 patients to be randomized, but this was subsequently revised because of slow recruitment as well as newer data from the INSTEAD trial. Finally 61 patients with acute uTBAD were randomized into cohorts of elective OMT+TEVAR to OMT alone. OMT was given to both arms of this study and the mortality at 30 days was zero. Given the small sample size and short duration of follow-up, the trial is not powered to detect differences in aortic-related and all-cause mortality. A recent meta-analysis demonstrates that there remains uncertainty whether TEVAR, in addition to OMT, is beneficial in acute and subacute uncomplicated type B aortic dissection. [31] The capability to accurately predict which patients with acute uTBAD will develop cTBAD could transform clinical management by allowing earlier intervention before complications occur.

## PREDICTORS OF DISSECTION RELATED EVENTS AFTER INITIAL CONSERVATIVE TREATMENT

Several prognostic predictors of dissection related events (dissection related death or need for intervention) after initial conservative treatment in acute uTBAD have previously been identified.

Predictors of complications in acute uTBAD during admission are aortic diameter ≥40mm, a primary entry tear >10mm, primary entry tear located on the concavity (undersurface) of the distal aortic arch and a FL diameter > 22mm. [31-34]

Prognostic predictors for dissection related events in acute TBAD during admission are a peak CRP level >96.1 mg/L and patency of the false lumen (defined as the concurrent presence of both flow and thrombus).

The peak CRP level is a strong predictor of long-term outcomes in acute uTBAD (Table II). [36] The peak CRP may represent the extent of the inflammatory reaction in the dissected aortic wall and may also reflect the damage to the lesion.

Patent false lumen and in particular partial thrombosis of the false lumen portends a poor outcome. [37] One potential explanation for a poor outcome relates the pressure within the false lumen to the presence of partial thrombosis. A patent false lumen may be perfused by a proximal

entry tear and decompressed by distal reentry tear(s), formation of a partial thrombus may occlude these distal tear(s), obstructing the outflow. An increase in pressure within the false lumen will increase wall tension, which may elevate the risk of aneurysm expansion, redissection and rupture.

Patients with complete thrombosis of the false lumen have improved outcomes, whereas those with a patent false lumen have an increased risk of aortic expansion and death. [6 33]

Antegrade flow through the false lumen is more likely to be associated with chronic false lumen patency than distal tears with retrograde flow. [38] Complete thrombosis of the false lumen excludes the false lumen from the circulation and is a predictor of less aortic enlargement and is related to lower mortality. Complete thrombosis of the false lumen is thought to be a prerequisite for complete healing.

**Tabel II.** Predictors of adverse dissections related events in ABAD

| | | | *HR* | *95% Confidence intervals* |
|---|---|---|---|---|
| At admission | Aortic diameter ≥40mm [6 34] | | 3.13 | 1.10 to 8.88 |
| | Primary entry tear >10mm [6 34] | | | |
| | Primary entry tear located on the concavity (undersurface) of the distal aortic arch [34 35] | | | |
| During admission | Peak CRP level [36] | 96.1 to 148.7 mg/L | 2.42 | 1.04 to 5.61 |
| | | 149.0 to 326.0 mg/L | 3.99 | 1.78 to 8.99 |
| | | FL diameter > 22mm [31 33] | | |
| | Patency of the false lumen [6 38] | | 7.63 | 2.68 to 21.69 |

## GENERAL OUTLINE AND AIM OF THE THESIS

Although some clinical and image based predictors of adverse outcomes have been identified there is still little basic mechanistic insight in the process of dissection and the behavior of the false lumen. Better understanding of important pathophysiologic elements of the dissection process can help to guide clinical management. This resulted in our interest to study the false lumen in TBAD. Improved understanding of the false lumen might result in new insights to predict and understand the development of dissection related adverse events in TBAD. The false lumen is influenced by dissection morphology, heamodynamics and aortic wall elasticity. An in-vitro or ex-vivo study has the potential to isolate and study one specific parameter in a controlled setting. Previous ex-vivo studies to examine dissection pathofysiology have used a non biological silicon tubing to simulate TBAD. For this thesis we created a porcine TBAD model and implemented it in a previously validated circulation system to have the ability to study several individual factors that influence the false lumen in TBAD.

In TBAD patent false lumen portends a poor outcome. Patent branch vessels originating from the false lumen in an aortic dissection type B are assumed to contribute to persistent blood flow and patent false lumen. Chapter 2 aims to assess the morphologic changes of the false lumen generated by different outflow rates in the created porcine TBAD model.

In contrast to aortic wall elasticity, the influence of haemodynamics and dissection morphology have been investigated often in multiple in-vitro and ex-vivo studies. Chapter 3 focuses on the influence of aortic wall elasticity on the diameter and pressure of the false lumen in aortic dissection by using the porcine TBAD model.

4D flow MRI has in contrast to the gold standard for imaging TBAD the ability to visualize and quantify flow and provide hemodynamic information such as wall shear stress. Chapter 4 examine the influence of heart rate on the volume, mean and peak wall shear stress by 4D flow MRI in the false lumen in the porcine aorta dissection model.

Fenestration is a minimally invasive alternative for the treatment of acute symptomatic TBAD because it may quickly decrease the pressure gradient of the false lumen. Chapter 5 evaluates were the optimal location of these fenestrations should be made.

## REFERENCE LIST


1. Nicholls F. Observations concerning the body of His Late Majesty, October 26, 1760. Phil Trans 1761;52:265–75
2. DeBakey ME, Cooley DA, Creech O Jr. Surgical considerations of dissecting aneurysm of the aorta. Ann Surg 1955;142 (4):586–612
3. Nienaber CA, Fattori R, Lund G, Dieckmann C, Wolf W, von KY, et al. Nonsurgical reconstruction of thoracic aortic dissection by stent-graft placement. N Engl J Med 1999 May 20;340(20):1539-45
4. Tiessen IM, Roach MR. Factors in the initiation and propagation of aortic dissections in human autopsy aortas. J Biomech Eng 1993 Feb;115(1):123-5.
5. McMahon MA, Squirrell CA. Multidetector CT of Aortic Dissection: A Pictorial Review. Radiographics 2010 Mar;30(2):445-60.
6. Riambau V, Böckler D , Brunkwall J, Cao P, et al. Management of Descending Thoracic Aorta Diseases. Eur J Vasc Endovasc Surg 2017 53 4-52
7. Dabbouseh NM, Ardelt A. Cocaine mediated apoptosis of vascular cells as a mechanism for carotid artery dissection leading to ischemic stroke. Med Hypotheses 2011 Aug;77(2):201-3
8. Michelena HI, Khanna AD, Mahoney D, Margaryan E, Topilsky Y, Suri RM, et al. Incidence of aortic complications in patients with bicuspid aortic valves. JAMA 2011 Sep 14;306(10):1104-12
9. Hiratzka LF, Bakris GL, Beckman JA, Bersin RM, Carr VF, Casey DE, Jr.. ACCF/AHA/AATS/ACR/ASA/SCA/SCAI/SIR/STS/SVM guidelines for the diagnosis and management of patients with Thoracic Aortic Disease: a report of the American College of Cardiology Foundation/American Heart Association Task Force on Practice Guidelines, American Association for Thoracic Surgery, American College of Radiology, American Stroke Association, Society of Cardiovascular Anesthesiologists, Society for Cardiovascular Angiography and Interventions, Society of Interventional Radiology, Society of Thoracic Surgeons, and Society for Vascular Medicine. Circulation 2010 Apr 6;121(13):e266-e369
10. Coady MA, Rizzo JA, Goldstein LJ, Elefteriades JA. Natural history, pathogenesis, and etiology of thoracic aortic aneurysms and dissections. Cardiol Clin 1999 Nov;17(4):615-35.
11. Suzuki T, Mehta RH, Ince H, Nagai R, Sakomura Y, Weber F, et al. Clinical profiles and outcomes of acute type B aortic dissection in the current era: lessons from the International Registry of Aortic Dissection (IRAD). Circulation 2003 Sep 9;108 Suppl 1:II312-II317.
12. Lombardi JV, Hughes GC, Appoo JJ, Bavaria JE et al. Society for Vascular Surgery (SVS) and Society of Thoracic Surgeons (STS) reporting standards for type B aortic dissections. J Vasc Surg 2020 Mar;71(3):723-747.
13. Klompas M. Does this patient have an acute thoracic aortic dissection? JAMA 2002 May 1;287(17):2262-72.
14. Kodolitsch von KY, Loose R, Ostermeyer J, Aydin A, Koschyk DH, Haverich A, et al. Proximal aortic dissection late after aortic valve surgery: 119 cases of a distinct clinical entity. Thorac Cardiovasc Surg 2000 Dec;48(6):342-6
15. Meredith EL, Masani ND. Echocardiography in the emergency assessment of acute aortic syndromes. Eur J Echocardiogr 2009 Jan;10(1):i31-i39
16. Khayat M, Cooper KJ, Khaja MS, Gandhi R, Bryce YC, Williams DM. Endovascular management of acute aortic dissection. Cardiovasc Diagn Ther. 2018;8(Suppl 1):S97-S107
17. Shiga T, Wajima Z, Apfel CC, Inoue T, Ohe Y. Diagnostic accuracy of transesophageal echocardiography, helical computed tomography, and magnetic resonance imaging for suspected thoracic aortic dissection: systematic review and meta-analysis. Arch Intern Med 2006 Jul 10;166(13):1350-6

18. Parodi J, Berguer R, Carrascosa P, Khanafer K, et al. Sources of error in the measurement of aortic diameter in computed tomography scans. J Vasc Surg 2014;59(1):74-9.
19. Amano Y, Sekine T, Suzuki Y, Tanaka K, Takagi R, Kumita S. Time-resolved three-dimensional magnetic resonance velocity mapping of chronic thoracic aortic dissection: a preliminary investigation. Magn Reson Med Sci 2011;10(2):93-9.
20. Wall Shear Stress: Theoretical Considerations and Methods of Measurement. Progress in Cardiovascular Diseases 2007 49;5 307-329
21. Liu Q, Lu JP, Wang F, Wang L, Tian JM. Three-dimensional contrast-enhanced MR angiography of aortic dissection: a pictorial essay. Radiographics 2007 Sep;27(5):1311-21
22. Tsai TT, Fattori R, Trimarchi S, Isselbacher E, Myrmel T, Evangelista A, et al. Long-term survival in patients presenting with type B acute aortic dissection: insights from the International Registry of Acute Aortic Dissection. Circulation 2006 Nov 21;114(21):2226-31
23. Midulla M, Renaud A, Martinelli T, Koussa M, Mounier-Vehier C, Prat A, et al. Endovascular fenestration in aortic dissection with acute malperfusion syndrome: immediate and late follow-up. J Thorac Cardiovasc Surg 2011 Jul;142(1):66-72.
24. Lombardi JV, Cambria RP, Nienaber CA, Chiesa R, Teebken O, Lee A, et al. Prospective multicenter clinical trial (STABLE) on the endovascular treatment of complicated type B aortic dissection using a composite device design. J Vasc Surg 2012 Mar;55(3):629-40
25. Chung J, Kasirajan K, Veeraswamy RK, Dodson TF, Salam AA, Chaikof EL, et al. Left subclavian artery coverage during thoracic endovascular aortic repair and risk of perioperative stroke or death. J Vasc Surg 2011 Jun 7
26. Nienaber CA, Kische S, Ince H, Fattori R. Thoracic endovascular aneurysm repair for complicated type B aortic dissection. J Vasc Surg 2011 Sep 12
27. Kodama K, Nishigami K, Sakamoto T, Sawamura T, Hirayama T, Misumi H, et al. Tight heart rate control reduces secondary adverse events in patients with type B acute aortic dissection. Circulation 2008 Sep 30;118(14 Suppl):S167-S170.
28. Nienaber CA, Rousseau H, Eggebrecht H, Kische S, Fattori R, Rehders TC, et al. Randomized comparison of strategies for type B aortic dissection: the INvestigation of STEnt Grafts in Aortic Dissection (INSTEAD) trial. Circulation 2009 Dec 22;120(25):2519-28
29. Brunkwall J, Kasprzak P, Verhoeven E, Heijmen R et al. Endovascular Repair of Acute Uncomplicated Aortic Type B Dissection Promotes Aortic Remodelling: 1 Year Results of the ADSORB Trial. Eur J Vasc Endovasc Surg. 2014 Sep;48(3):285-91.
30. Nienaber CA, Kische S, Rousseau H, et al. Endovascular repair of type B aortic dissection: long-term results of the randomized investigation of stent grafts in aortic dissection trial. Circ Cardiovasc Interv 2013;6:407–16
31. Hossack M, Patel S, Gambardella I, Neequaye et al. Endovascular vs. Medical Management for Uncomplicated Acute and Sub-acute Type B Aortic Dissection: A Meta-analysis. Eur J Vasc Endovasc Surg 2020 May;59(5):794-807
32. Sakakura K, Kubo N, Ako J, Fujiwara N, Funayama H, Ikeda N, et al. Determinants of long-term mortality in patients with type B acute aortic dissection. Am J Hypertens 2009 Apr;22(4):371-7.
33. Spinelli D, Benedetto F, Donato R, Piffaretti G et al. Current evidence in predictors of aortic growth and events in acute type B aortic dissection. J Vasc Surg 2018 Dec;68(6):1925-1935.e8
34. Takahashi J, Wakamatsu Y, Okude J, Kanaoka T, Sanefuji Y, Gohda T, et al. Maximum aortic diameter as a simple predictor of acute type B aortic dissection. Ann Thorac Cardiovasc Surg 2008 Oct;14(5):303-10
35. Tolenaar JL, van Keulen JW, Jonker FH, et al. Morphologic predictors of aortic dilatation

in type B aortic dissection. J Vasc Surg 2013 Nov;58(5):1220-5.

36. Sakakura K, Kubo N, Ako J, Wada H, Fujiwara N, Funayama H, et al. Peak C-reactive protein level predicts long-term outcomes in type B acute aortic dissection. Hypertension 2010 Feb;55(2):422-9
37. Tsai TT, Evangelista A, Nienaber CA, Myrmel T, Meinhardt G, Cooper JV, et al. Partial thrombosis of the false lumen in patients with acute type B aortic dissection. N Engl J Med 2007 Jul 26;357(4):349-59.
38. Sueyoshi E, Sakamoto I, Hayashi K, Yamaguchi T, Imada T. Growth rate of aortic diameter in patients with type B aortic dissection during the chronic phase. Circulation 2004 Sep 14;110(11 Suppl 1):II256-II261

# 2

# The Role of Branch Vessels in Aortic Type B Dissection An In-vitro Study

H.T.C. Veger
J.J.M. Westenberg
M.J.T. Visser

European Journal of Vascular and Endovascular Surgery. 2015

## ABSTRACT

### Objective

In Acute type B Aortic Dissection (ABAD) patent false lumen portends a poor outcome. Patent branch vessels originating from the false lumen in an aortic dissection type B are assumed to contribute to persistent blood flow and patent false lumen. Therefore we studied the morphologic changes of the false lumen generated by different outflow rates in an in-vitro model.

### Materials and Methods

An artificial dissection was created in two ex-vivo porcine aortas. A thin cannula was placed in the false lumen simulating a branch vessel originating from the false lumen. The aorta was positioned in a validated in-vitro circulatory system with physiological pulsatile flow (1500-2700ml/min) and pressure characteristics (130/70mmHg). The cannula was attached to a small silicone tube with an adjustable valve mechanism. Three different valve settings were used for creating outflow of the false lumen (fully closed, opened at 50% and fully opened at 100%). With time-resolved Magnetic Resonance Imaging measurements of lumen areas and flow rates were assessed. The experiment was performed twice in two different porcine aortas with a similar morphology in order to study reproducibility.

### Results

Increasing antegrade outflow through the branch vessel of the false resulted in a significant ($p < 0.01$) increase of the mean false lumen area at the proximal and distal location in both models. The distal false lumen expanded up to 107% in case of high outflow of the false lumen through the branch vessel.

### Conclusion

In this in-vitro study, we showed that increasing antegrade outflow through branch vessel originating from the false lumen when no distal re-entry tear is present results in an expansion of the cross-sectional false lumen area.

## INTRODUCTION

Uncomplicated Acute type B Aortic Dissection (ABAD) is still associated with a 30-day mortality of approximately 10%.[1] Although the introduction of thoracic endovascular aneurysm repair (TEVAR) showed promising results in complicated ABAD, best medical treatment (BMT) is still todays treatment for uncomplicated ABAD. The acutely dissected aorta is fragile and TEVAR can result in malperfusion, ischemia, retrograde dissection, rupture and finally even perioperative mortality. The results of the ADSORB trial, as the first randomised comparison between acute (< 14 days) endovascular surgery and BMT for uncomplicated ABAD, showed only that aortic remodelling after one year was in favour of endograft placement. The ADSORB trial did not show an improved 1 year survival rate (although not powered for survival).[2]. The INSTEAD trial, as the first randomized comparison between elective endovascular surgery and BMT, justified medical management in the early phase for uncomplicated chronic ABAD from 2 to 52 weeks of onset.[1] For stable survivors of acute type B dissection, benefits of TEVAR begin to show after 2 years of follow-up.[3, 4] Although the preliminary results of the uncompleted ABSORB trial did not show any beneficial effect of early TEVAR, theoretically early TEVAR might save the lives of around 10% of patients, minus the induced perioperative mortality by TEVAR, with initially uncomplicated ABAD treated with BMT.[2] Therefore, identification of clinical and imaging predictors of poor prognosis in uncomplicated ABAD seems mandatory to select patients who will benefit from early TEVAR.

In the acute ABAD the false lumen may remain patent, thrombose, recommunicate with the true lumen through fenestrations, or rupture. Complete false lumen thrombosis is a major predictor of prognosis because it excludes the false lumen from the circulation and is thought to be a prerequisite for complete healing in the long run.[5,6] Incomplete thrombosis or patent false lumen portends a poor outcome.[7-9] The occurrence of thrombosis in the false lumen depends on coagulability, endothelial injury/dysfunction and blood flow. The blood flow in the false lumen is highly variable due to morphological differences between various types of dissections.[10] It is conceivable that patent branch vessels originating from the false lumen in an aortic dissection type B may contribute to persistent blood flow and patent false lumen, and thus to prognosis. Therefore, an in-vitro study was performed using two ex-vivo porcine aortas, both with a surgically-constructed false lumen and an adjustable outflow branch. We studied the morphologic changes of the false lumen generated by different outflow rates and hypothesize that increased outflow through the branch vessel originating from the false lumen will result in an increase of the false lumen.

# MATERIALS AND METHODS

## Aortic dissection model

Two fresh porcine aortas were obtained from the abattoir and within 4 hours prepared as follows: from the aortic arch to the iliac bifurcation all side branches were ligated with prolene 5.0. At the descending aorta a transverse semi-circular incision was made though all vessel layers and a dissection was surgically created in the media layer resulting in a false and true lumen with a dissection flap. The surgically created false lumen in the media may be considered comparable to a human aortic dissection (Figure 1). A thin plastic cannula (diameter of 2 mm) was placed in the false lumen simulating a branch vessel originating from the false lumen. The morphology of both models is representative for an aortic dissection type B with no distal tear or partial thrombosis occluding distal tears, impending outflow resulting in a blind sac from where a single branch vessel originates (Figure 2). The models were stored in a refrigerator for approximately 48 hours and subsequently defrozen before the start of the experiments.

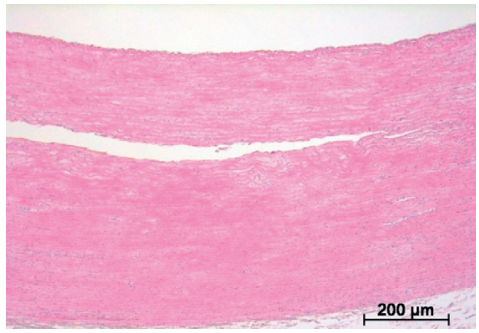


**Figure 1.** Microscopy after hematoxylin and eosin staining for the histological evaluation of the artificially created false lumen. The false lumen is created between intima with partial thickness media and partial thickness media with adventitia.

The cannula simulating a branch vessel was attached to a small silicone tube with an adjustable valve mechanism enabling a setting of variable outflow rates. Three different valve settings were used: fully closed, opened at 50% and fully opened at 100% for creating antegrade outflow of the false lumen. Magnetic Resonance Imaging (MRI) measurements were performed (details are given below) at four equidistantly spaced locations (32 mm apart) and perpendicular to the aortic model: proximally to the dissection, at the beginning of the dissection, half way of the dissection and distally to the dissection. A schematic representation of the models and measurement locations is presented in Figure 2**.**

In Model 1 data were acquired first with the valve setting fully closed, next opened at 50% and then fully opened at 100%. For Model 2, data was acquired with valve settings in inverse order, preventing a potential bias due to the duration of the experiment.

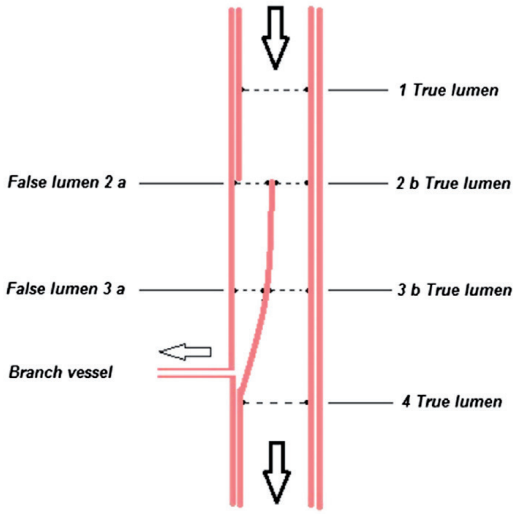


**Figure 2.** A schematic representation of the model. The four imaging planes are indicated and the arrows represent the flow direction.

## In-vitro circulatory system

A validated in-vitro circulatory system with physiological flow and pressure characteristics was used to simulate the human circulatory system.[11-13] The main components of this circulatory system are: a pneumatically-**driven** pulsatile pump with periodic triggering connecting to the MRI system for synchronization, simulating ECG-triggering, a compliance chamber and a watertight synthetic box with the aortic dissection model (Figure 3). All components are connected by a silicone tubing system. The flow depends on the resistance in the in-vitro model and varies from 1500-2700ml/min. Water doped with a low concentration of gadolinium-based contrast (Dotarem, Guerbet) to shorten T1 relaxation time was used as circulating fluid. During the experiments the pneumatically-**driven** pulsatile pump was set on a fixed frequency of 68 beats/minute and at the start of each beat, a trigger was produced by the triggering unit connected to the MRI system. The pressure of the circulated water was 130/70mmHg and was calibrated several times.

The synthetic box with the aortic dissection model was placed inside the MRI gantry and filled with water, resulting in a submerged aortic dissection model. The antegrade outflow through the simulated branch originating from the false lumen vessel was redirected to the main reservoir.

## Imaging

Time-resolved multi-slice two-dimensional imaging was performed with a 1.5T MRI system (Gyroscan, Philips Medical Systems, Best, The Netherlands) at four equidistantly spaced locations perpendicularly positioned to the aorta model as indicated in Figure 2. The spatial resolution used in the MRI protocol was $1.2 \times 1.2 mm^2$. Phase-contrast velocity-encoding was performed, resulting in both anatomical images and velocity images of the through-plane flow. Specific imaging parameters

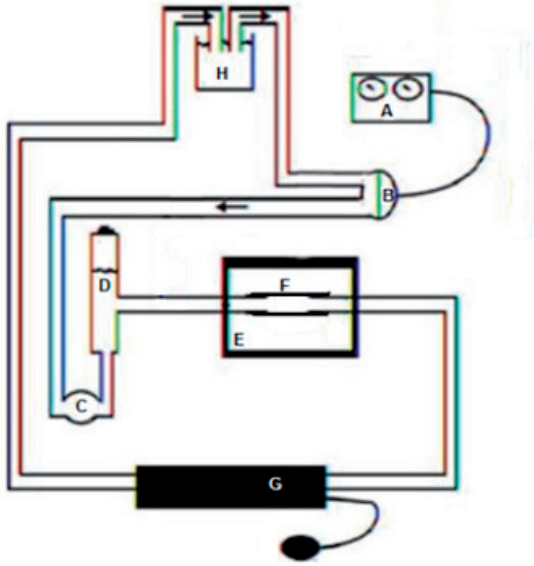


**Figure 3.** Circulation set up. A schematic representation of the circulation set up, which consisted of (A) an artificial pneumatic heart driver, (B) a tube to left ventricle, (C) a left ventricle, (D) a silicon tube, (E) a ball valve, (F) an air chamber, (G) the aortic dissection model (see Fig. 2), (H) a watertight synthetic box, (I) a blood pressure cuff, and (J) an open reservoir.

were: echo time 3.0ms, repetition time 5.0ms, flip angle 20°, slice thickness 8mm, field-of-view 300×150mm$^2$, two signal averages and velocity-encoding with sensitivity of 120 cm/s. Retrospective gating was used with a total of 160 phases reconstructed. Image analysis was performed using in-house developed and validated software and manual contour segmentation. [15] Cross-sectional area distention of the aorta was determined from the anatomical images acquired at each location. Therefore, the lumen area of both the true and false lumen were manually segmented in each phase of the cardiac cycle for a total of 160 phases. Lumen area (in mm$^2$) versus time-graphs were determined.

## Statistical analysis

The cross-sectional lumen area (in mm$^2$) at all four locations in the aortic dissection model (Figure 2) were determined for all three valve settings, creating different false luminal outflow. Paired t-tests were used to determine statistical significance in lumen area change at each location in the aortic dissection model during different false luminal outflow. Statistical significance was assumed at $P < .05$.

## RESULTS

The general flow characteristics of the in-vitro circulation in both models are presented in Table 1. Both models had a similar morphology but differed in lumen diameter resulting in a different vascular resistance and thereby resulting in different general flow characteristics (Table 1 and 2). The mean cross-sectional lumen area proximal to the dissection increased when the outflow settings were adjusted in model 1 but not in model 2 (Table 2).

**Table 1.** General flow characteristics for models 1 and 2.

| *In vitro* circulatory system flow characteristics | | | |
|---|---|---|---|
| | | Model 1 | Model 2 |
| Heart beat/min | | 68 | 68 |
| Mean stroke volume/beat | | 40 mL | 21.5 mL |
| Stroke volume/min | | 2,720 mL | 1,460 mL |
| False lumen outflow/min | Valve setting Closed | | |
| | 50% | 31 mL | 24 mL |
| | 100% | 86 mL | 58 mL |

**Table 2.** Data summary of mean ± SD lumen area for the three different outflow conditions in models 1 and 2

| Outflow by branch vessel vs. false lumen area | | | | | | | |
|---|---|---|---|---|---|---|---|
| Scan plane area | Outflow by branch vessel | Model 1 | | | Model 2 | | |
| | | 0 | 0.5 mL/beat | 1.3 mL/beat | 0 | 0.5 mL/beat | 0.9 mL/beat |
| True lumen 1 | | 249.4 ± 38.0 | 274.1 ± 15.4 | 274.0 ± 15.3 | 159.6 ± 3.8 | 165.3 ± 16.6 | 150.3 ± 18.6 |
| False lumen 2 A ($mm^2$) | | 70.3 ± 32.2 | 72.9 ± 31.7 | 75.3 ± 25.6 | 11.2 ± 8.9 | 14.8 ± 10.3 | 22.9 ± 11.9 |
| True lumen 2 B ($mm^2$) | | 198.3 ±11.2 | 187.6 ± 7.3 | 179.2 ± 13.7 | 157.2 ± 13.9 | 159.3 ± 14.1 | 151.9 ± 21.9 |
| False lumen 3 A ($mm^2$) | | 46.5 ± 8.2 | 52.2 ± 5.8 | 56.7 ± 5.7 | 10.2 ± 6.2 | 13.4 ± 8.8 | 21.1 ± 14.8 |
| True lumen 3 B ($mm^2$) | | 180.1 ± 21.4 | 173.3 ± 18.7 | 165.8 ± 18.6 | 137.7 ± 15.1 | 143.2 ± 11.6 | 137.8 ± 12.2 |
| True lumen 4 ($mm^2$) | | 165.7 ± 41.5 | 190.8 ± 38.6 | 186.9 ± 40.4 | 125.4 ± 14.9 | 128.3 ± 15.5 | 120.9 ± 13.9 |

The proximal imaging plane was positioned at the opening of the dissection at location 2 (Figure 2). At this location, the cross-sectional area of the false lumen in model 1 expanded with more than 7% (70.3$mm^2$ to 75.3$mm^2$; Figure 4) when the outflow of the false lumen increased to 3.3% of the mean stroke volume (1.3ml/beat versus 40ml mean stroke volume). In model 2 the cross-sectional area of the false lumen at the distal location (i.e., location 3) expanded with more than 104% (11.2$mm^2$ to 22.9$mm^2$; Figure 5 and 6) when the outflow of the false lumen was increased to 4.2% of the mean stroke volume (0.9ml/beat versus 21.5ml stroke volume).

Increasing the outflow through the branch vessel of the false lumen resulted in an increase of the mean cross-sectional false lumen area in both models (Figure 4 and 5), which was statistically significant ( $P < .05$) for the three outflow settings. The range in lumen area changed during the three different outflow conditions with the largest range observed in model 2 (Figure 4 and 5).

In the proximal acquisition plane of the true lumen, the mean cross-sectional lumen area changed for the three different outflow conditions (2 B, Figure 2), however no correlation was found (Table 2.).

Distally in the false lumen (3A, Figure 2), an increase in mean lumen area was measured when the outflow of the false lumen was adjusted (Figure 4 and 5). This increase is statistically significant ( $P < .05$) for the three outflow settings in both models. The distal false lumen area in model 1 expanded with more than 21% (46.5mm$^2$ to 56.7mm$^2$; Figure 4) when the outflow of the false lumen was increased to 3.3% of the mean stroke volume (1.3ml/beat versus 40ml mean stroke volume). In model 2 the distal false lumen area expanded with more than 107% (10.2mm$^2$ to 21.1mm$^2$; Figure 5) when the outflow of the false lumen was increased to 4.2% of the mean stroke volume (0.9ml/beat versus 21.5ml stroke volume). The range of the lumen area remains consistent for the three different outflow conditions in model 1 but showed an increase in model 2 (Figure 4 and 5).

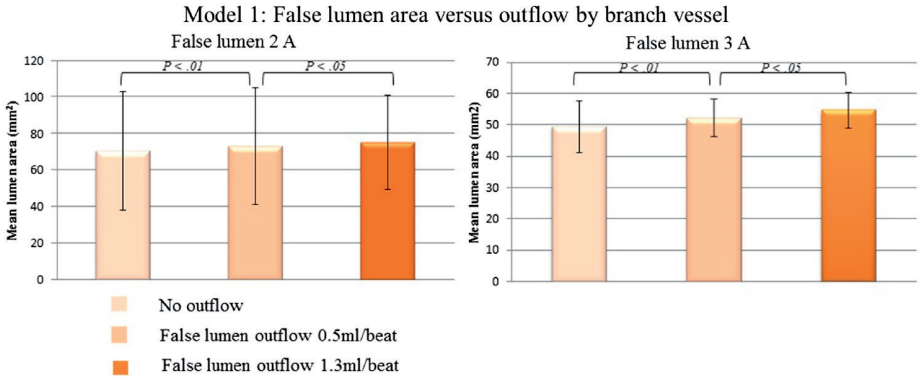


**Figure 4.** Model 1. The mean ± SD area of the proximal and distal plane in the false lumen for the three different outflow conditions. False lumen outflow result in significant area increase of the false lumen (2A and 3A).

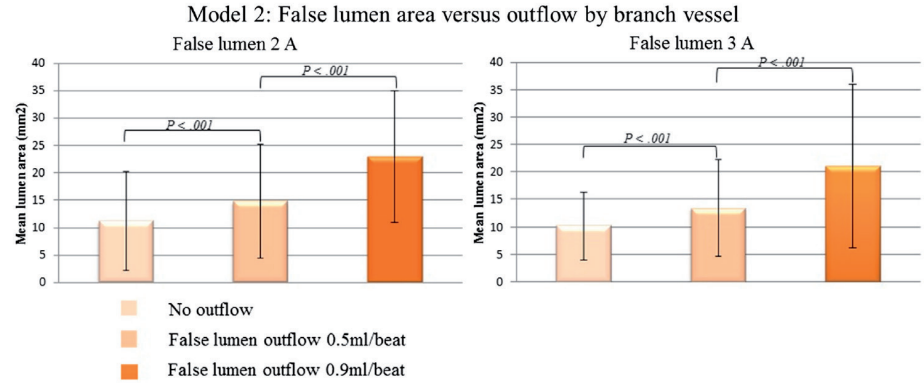


**Figure 5.** Model 2. The mean ± SD area of the proximal and distal plane in the false lumen for the three different outflow conditions. False lumen outflow result in significant area increase of the false lumen (2A and 3A).

For the distal acquisition plane (3 B, Figure 2), a statistically significant decrease ($p < 0.01$) of the mean lumen area of the true lumen was measured in model 1 when the outflow of the false lumen was increased (Table 2.). In model 2, the measured true lumen area remained stable at the highest false luminal outflow (Table 2.).

For both models, the mean lumen area measured in the acquisition plane 4 distalto the dissection (4, Figure 2) changed during the three different outflow conditions, however no correlation was found.

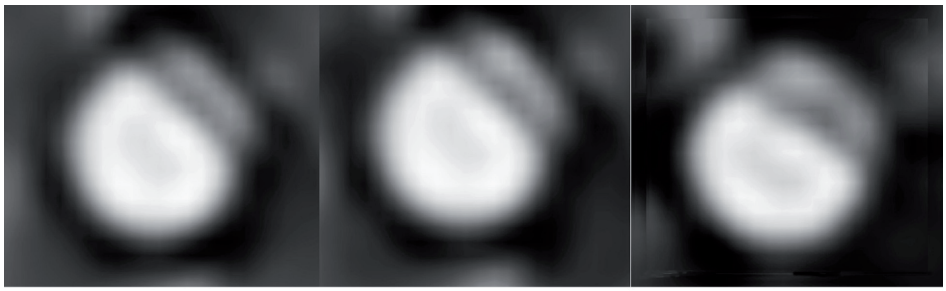


**Figure 6.** Magnetic resonance angiography images at the same cardiac phase of the distal false lumen in model 2 visualizing the expansion of the false lumen. (A) No outflow; (B) outflow 0.5 mL/second; (C) outflow 0.9 mL/second.

## DISCUSSION

Patients with uncomplicated ABAD have an overall in-hospital mortality of around 10% despite best medical treatment. [7, 16, 17] Once complications occur the prognosis declines, with hospital mortality greater than 50%.[18] Early TEVAR might save theoretically the lives of around 10% of patients with initially uncomplicated ABAD although the preliminary results of the uncompleted ABSORB trial did not show any beneficial effect of early TEVAR. [2 19]

Therefore, identification of clinical and imaging predictors of poor prognosis in uncomplicated ABAD seems mandatory to select patients who will benefit from early TEVAR. Although theoretically saving lives the opposite effect of TEVAR is the procedure induced complications like malperfusion, ischemia, retrograde dissection, rupture and finally even perioperative mortality.

Complete false lumen thrombosis in ABAD excludes the false lumen from the circulation and is a major predictor of prognosis.[5, 6] However, ABAD with patent false lumen including partial thrombosis presents a high risk of complications. [9, 20, 21] The occurrence of incomplete thrombosis will depend on the presence of flow in the false lumen which is maintained by outflow of patent branch vessel(s) and / or fenestrations including re-entries of the dissection flap. Outflow by patent branch vessel(s) results in continuing flow in the false lumen and may contribute to adverse events. We hypothesized that increased outflow by branch vessels originating from the false lumen

results in a larger false lumen. To study this hypothesis an in-vitro study with circulatory flow was performed in which ex-vivo porcine aortas were included with a surgically-constructed false lumen and to which a branch vessel was added originating from the false lumen with an adjustable outflow, representing an uncomplicated ABAD (Figure 2). To validate reproducibility of our results, the experiment was performed in two different porcine aortas with similar morphology.

Ex-vivo models are useful for studying haemodynamics of aortic pathologies, as individual factors in a complicated circulation system can be isolated and analysed. In this study, we applied a porcine aorta as 'modelled' aorta, replacing the synthetic polymer or silicon tubing used in previous in-vitro studies. [22, 23] Additionally we used MRI (including simulating ECG-triggering synchronization) for time-resolved imaging, which was not described previously in in-vitro studies. [22-25] The presented porcine aorta model morphology is representative for dissections with no distal tear or with partial thrombosis occluding distal tears, impending outflow resulting in a blind sac.[20]

Our model confirmed that the cross-sectional area of the false lumen expanded when outflow of the false lumen was present through a branch vessel originating from the false lumen. The expansion of the false lumen was observed in both models and in both acquisition planes of the false lumen, proximal and distal in the dissection. The largest expansion was observed in the distal location of the false lumen in model 2, with an area expansion of more than 107%.

Translation of the results from our in-vitro model to a physiological situation is of course limited and therefore, evaluation of patients should be performed to confirm our findings. Additionally, in part due to limitations inherent to replicating in vivo conditions, preclinical testing has a limited ability in reproducing clinical settings.[25] Therefore, following limitations of the pulsatile flow model need to be acknowledged: water was used as a circulatory medium instead of blood, which is a thrombotic medium. Spontaneous thrombosis could either block the tubing system or disturb the function of the pulsatile pump.[24] The applied pulsatile flow was not equal to an aortic flow. Also, the aortas were prepared, frozen and after two days de-frozen. This might have altered the elastic properties of the arterial wall. Furthermore, the absence of dissected lamella might have influenced the outflow vessel. Implementation of lamella in a model would be too complex and would result in many variables. Next, the aortic model was submerged in water without support, which is not be representative for the connective tissue normally surrounding the aorta. Next, only two porcine aortic models were used in the experiments and more aortic models would result in more accurate data. Finally, we studied a small spectrum of outflow by branch vessel originating from the false lumen although these outflow settings already resulted in a significant increase of the false lumen area.

In conclusion, our in-vitro study showed that outflow through a branch vessel originating from the false lumen in an aortic dissection results in expansion of cross-sectional false lumen area. False lumen expansion might result in higher stress in the aortic wall, increasing the risk of dilatation which contributes to the conversion of uncomplicated into complicated ABAD. Our findings suggest that initially uncomplicated ABADs with no distal entry tear, but patent branch vessels

originating from the false lumen, have a higher risk for complications and that in such cases, early TEVAR may be considered.

## REFERENCE LIST


(1) Nienaber CA, Zannetti S, Barbieri B, Kische S, Schareck W, Rehders TC. INvestigation of STEnt grafts in patients with type B Aortic Dissection: design of the INSTEAD trial--a prospective, multicenter, European randomized trial. Am Heart J 2005 Apr;149(4):592-9.

(2) Brunkwall J, Lammer J, Verhoeven E, Taylor P. ADSORB: a study on the efficacy of endovascular grafting in uncomplicated acute dissection of the descending aorta. Eur J Vasc Endovasc Surg 2012 Jul;44(1):31-6.

(3) Nienaber CA, Kische S, Rousseau H, Eggebrecht H, Rehders TC, Kundt G, et al. Endovascular repair of type B aortic dissection: long-term results of the randomized investigation of stent grafts in aortic dissection trial. Circ Cardiovasc Interv 2013 Aug;6(4):407-16.

(4) Fattori R, Montgomery D, Lovato L, Kische S, Di EM, Ince H, et al. Survival after endovascular therapy in patients with type B aortic dissection: a report from the International Registry of Acute Aortic Dissection (IRAD). JACC Cardiovasc Interv 2013 Aug;6(8):876-82.

(5) Tsai TT, Evangelista A, Nienaber CA, Myrmel T, Meinhardt G, Cooper JV, et al. Partial thrombosis of the false lumen in patients with acute type B aortic dissection. N Engl J Med 2007 Jul 26;357(4):349-59.

(6) Clough RE, Hussain T, Uribe S, Greil GF, Razavi R, Taylor PR, et al. A new method for quantification of false lumen thrombosis in aortic dissection using magnetic resonance imaging and a blood pool contrast agent. J Vasc Surg 2011 Nov;54(5):1251-8.

(7) Tsai TT, Evangelista A, Nienaber CA, Myrmel T, Meinhardt G, Cooper JV, et al. Partial thrombosis of the false lumen in patients with acute type B aortic dissection. N Engl J Med 2007 Jul 26;357(4):349-59.

(8) Evangelista A, Salas A, Ribera A, Ferreira-Gonzalez I, Cuellar H, Pineda V, et al. Long-term outcome of aortic dissection with patent false lumen: predictive role of entry tear size and location. Circulation 2012 Jun 26;125(25):3133-41.

(9) Tanaka A, Sakakibara M, Ishii H, Hayashida R, Jinno Y, Okumura S, et al. Influence of the false lumen status on short- and long-term clinical outcomes in patients with acute type B aortic dissection. J Vasc Surg 2013 Oct 16.

(10) Karmonik C, Bismuth J, Redel T, Anaya-Ayala JE, Davies MG, Shah DJ, et al. Impact of tear location on hemodynamics in a type B aortic dissection investigated with computational fluid dynamics. Conf Proc IEEE Eng Med Biol Soc 2010;2010:3138-41.

(11) Hinnen JW, Koning OH, Vlaanderen E, van Bockel JH, Hamming JF. Aneurysm sac pressure monitoring: effect of pulsatile motion of the pressure sensor on the interpretation of measurements. J Endovasc Ther 2006 Apr;13(2):145-51.

(12) Bosman WM, van der Steenhoven TJ, Hinnen JW, Kaptein BL, de Vries AC, Brom HL, et al. Aortic customize: a new alternative endovascular approach to aortic aneurysm repair using injectable biocompatible elastomer. An in vitro study. J Vasc Surg 2010 May;51(5):1230-7.

(13) Hinnen JW, Koning OH, Vlaanderen E, van Bockel JH, Hamming JF. Aneurysm sac pressure monitoring: effect of pulsatile motion of the pressure sensor on the interpretation of measurements. J Endovasc Ther 2006 Apr;13(2):145-51.

(14) Rengier F, Geisbusch P, Vosshenrich R, Muller-Eschner M, Karmonik C, Schoenhagen P, et al. State-of-the-art aortic imaging: part I - fundamentals and perspectives of CT and MRI. Vasa 2013 Nov;42(6):395-412.

(15) van der Geest RJ, de RA, van der Wall EE, Reiber JH. Quantitative analysis of cardiovascular MR images. Int J Card Imaging 1997 Jun;13(3):247-58.

(16) Hagan PG, Nienaber CA, Isselbacher EM, Bruckman D, Karavite DJ, Russman PL, et al.

The International Registry of Acute Aortic Dissection (IRAD): new insights into an old disease. JAMA 2000 Feb 16;283(7):897-903.

(17) Suzuki T, Mehta RH, Ince H, Nagai R, Sakomura Y, Weber F, et al. Clinical profiles and outcomes of acute type B aortic dissection in the current era: lessons from the International Registry of Aortic Dissection (IRAD). Circulation 2003 Sep 9;108 Suppl 1:II312-II317.

(18) Fattori R, Mineo G, Di EM. Acute type B aortic dissection: current management strategies. Curr Opin Cardiol 2011 Nov;26(6):488-93.

(19) Brunkwall J(1) KP2HR3VE4AP5vT-KH6aTP7. ADSORB- a Prospective Randomised Controlled Trial in Acute Uncomplicated Type B Dissection: Stent Graft Induces False Channel Thrombosis and Reduces its False Lumen Size - 1 Year Results. 2012.

(20) Tsai TT, Evangelista A, Nienaber CA, Myrmel T, Meinhardt G, Cooper JV, et al. Partial thrombosis of the false lumen in patients with acute type B aortic dissection. N Engl J Med 2007 Jul 26;357(4):349-59.

(21) Evangelista A, Salas A, Ribera A, Ferreira-Gonzalez I, Cuellar H, Pineda V, et al. Long-term outcome of aortic dissection with patent false lumen: predictive role of entry tear size and location. Circulation 2012 Jun 26;125(25):3133-41.

(22) Chung JW, Elkins C, Sakai T, Kato N, Vestring T, Semba CP, et al. True-lumen collapse in aortic dissection: part II. Evaluation of treatment methods in phantoms with pulsatile flow. Radiology 2000 Jan;214(1):99-106.

(23) Tsai TT, Schlicht MS, Khanafer K, Bull JL, Valassis DT, Williams DM, et al. Tear size and location impacts false lumen pressure in an ex vivo model of chronic type B aortic dissection. J Vasc Surg 2008 Apr;47(4):844-51.

(24) Qing KX, Chan YC, Lau SF, Yiu WK, Ting AC, Cheng SW. Ex-vivo haemodynamic models for the study of Stanford type B aortic dissection in isolated porcine aorta. Eur J Vasc Endovasc Surg 2012 Oct;44(4):399-405.

(25) Faure EM, Canaud L, Cathala P, Serres I, Marty-Ane C, Alric P. Human ex-vivo model of Stanford type B aortic dissection. J Vasc Surg 2013 Sep 20.

# 3

# The Influence of Aortic Wall Elasticity on the False Lumen in Aortic Dissection An in-vitro study

H.T.C. Veger
E.H. Pasveer
J.J.M. Westenberg
J.J. Wever
R.G. Statius van Eps

Vascular and Endovascular Surgery. 2020

## ABSTRACT

### Background

Haemodynamics, dissection morphology and aortic wall elasticity have a major influence on the pressure in the false lumen. In contrast to aortic wall elasticity, the influence of haemodynamics and dissection morphology have been investigated often in multiple in-vitro and ex-vivo studies. The purpose of this study was to evaluate the influence of aortic wall elasticity on the diameter and pressure of the false lumen in aortic dissection.

### Methods

An artificial dissection was created in three ex vivo porcine aortas. The aorta models were consecutively positioned in a validated in vitro circulatory system with physiological pulsatile flow. Each model was imaged with ultrasound on four positions along the aorta and the dissection. At these four locations, also pressure measurement were performed in the true and false lumen with an arterial catheter. After baseline experiments the aortic wall elasticity was adjusted with silicon and the experiments were repeated.

### Results

The aortic wall elasticity was decreased in all three models after siliconizing. In all three siliconized models the diameters of the true and false lumen increased at proximal, mid and distal location while the mean arterial pressure did not significantly change.

### Conclusions

In this in-vitro study, we showed that aortic wall elasticity is an important parameter altering the false lumen. An aortic wall with reduced elasticity results in an increased false lumen diameter in the mid and distal part of the false lumen. These results can only be transferred to corresponding clinical situations to a limited extent.

## INTRODUCTION

Consensus has been established to manage uncomplicated Acute type B Aortic Dissection (ABAD) in the acute phase (0-2 weeks) with surveillance and optimal medical treatment (OMT) with control of hypertension and heart rate.[1] The reported 30 days in hospital mortality of an uncomplicated ABAD is 2.4%, but when an uncomplicated ABAD converts to a complicated ABAD the 30 days in hospital mortality quadruples.[2] In the subacute phase of an uncomplicated ABAD with suitable anatomy there is increasing evidence of improved survival and less progression of disease at 5 years after elective Thoracic EndoVascular Aortic Repair (TEVAR).[3,4] Gaining more insight in the false lumen behaviour of the acute uncomplicated ABAD may result in identifying those patients who are at high risk of developing complications and may benefit from elective TEVAR in the acute phase.

Aortic dissection is defined as a pathological condition characterized by the presence of an aortic intimal tear and medial dissection, in which blood flows from the entry site into the false lumen.[5] Haemodynamics, dissection morphology and aortic wall elasticity have a major influence on the pressure in the false lumen.[6] In contrast to the aortic wall elasticity, the influence of haemodynamics and dissection morphology have been investigated often in multiple in-vitro and ex-vivo studies.[7,8] Aortic wall elasticity is variable and often altered in aortic dissections.[9,10] The aortic wall elasticity can be influenced by aging and atherosclerosis.[11]

Today's literature on the influence of aortic wall elasticity on the pressure of the false lumen consists of only one in-vitro study using a lumped parameter model.[12] This study described the role of wall elasticity as a determinant of intraluminal pressures and flow patterns.[12] Additional research is needed to better understand the role of aortic wall elasticity and its relation to false lumen diameter and false lumen pressure characteristics in uncomplicated ABAD. We hypothesize that a less elastic aortic wall will result in an increase of false lumen pressure and diameter. We studied this hypothesis by adjusting the aortic wall elasticity in a validated in-vitro porcine aorta dissection model in a pulsatile flow-model.

## MATERIALS AND METHODS

### Aortic dissection model

To create a porcine Type B Aortic Dissection model with patent false lumen, we used a technique that was previously described by Qing et al.[12] Fresh porcine aortas were obtained frozen from the abattoir. The porcine aortas were defrosted and prepared as following: from the aortic arch to the iliac bifurcation all side branches were ligated with 5.0 Prolene. The porcine aorta was everted with the help of a clamp. Before starting, orifices of small branches on the intimal surface were observed, and the route of creating the dissection flap was carefully planned. [13] A 24-GA I.V. catheter was used to puncture the intima till mid-portion of media, and approximately 10cc of

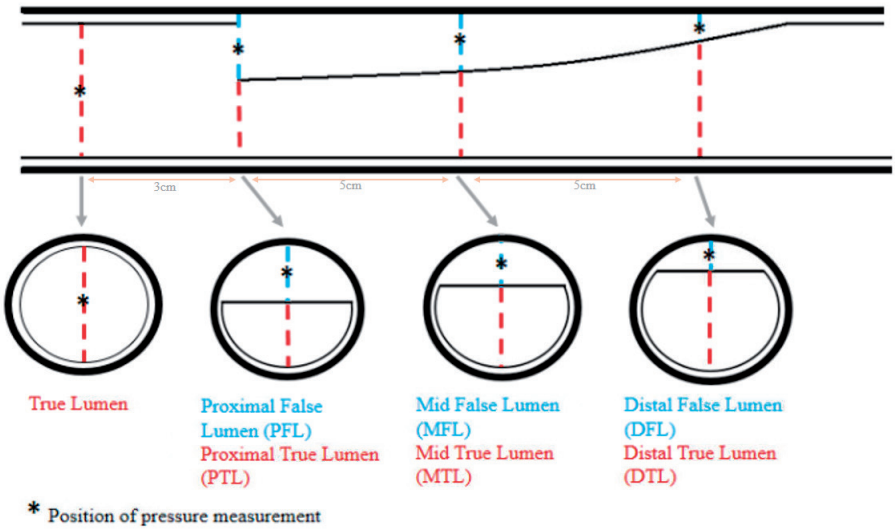


**Figure 1.** Schematic overview of the aortic dissection model. The four imaging planes and pressure measurement positions are presented.

saline was injected, creating an intramural haematoma.[13] The dissection was extendend by both injecting saline and pressing the bleb without rupturing the dissection flap resulting in a dissection with a length of 11cm. Subsequently, the dissection flap was cut in a proximal location to create a primary entry. Finally, the aorta was everted back to finish the procedure. The dissection area was longitudinally divided in proximal, mid and distal (Figure 1). A total of three aortic dissection models with all similar morphology, a primary entry tear and a dissection length of 11 cm were made (Figure 1). After baseline experiments (see below) the aortic wall elasticity of each aortic model was adjusted by applying a synthetic polymer made up of silicon to the outer layer of the aortic model (Silicone, Bison, The Netherlands) and the experiment was repeated. The basis to choose for this method of siliconizing was to achieve a more rigid aortic wall as can be seen by aging and atherosclerosis.[11] The effect of siliconizing the outer wall was evaluated by measuring the lumen diameter under flow conditions prior to the dissection. Approval of the Institutional Review Board (IRB) was not needed because no animals were sacrificed for this study.

## In-vitro circulatory system

A validated in-vitro circulatory system with physiological flow and pressure characteristics was used to mimic the human circulatory system.[14,15,16] The main components of this circulatory system are a pneumatically-driven pulsatile pump, a compliance chamber and the watertight synthetic box with the aortic dissection model (Figure 2). All components are connected by a silicone tubing system and water was used for circulating fluid. During the experiments the pneumatically-driven pulsatile pump was set on normotensive (pressure 130/70mmHg; Mean Arterial Pressure – MAP

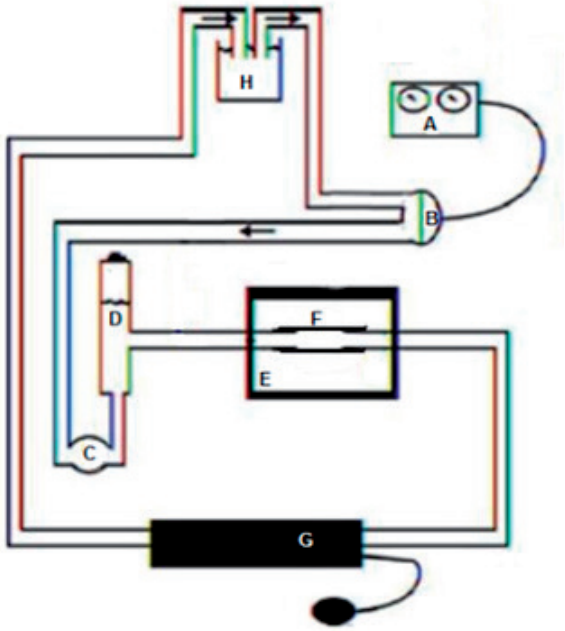


**Figure 2.** Circulation set-up. A schematic representation of the circulation set-up, which consisted of an artificial heart driver (A), left ventricle (B), a ball valve (C), an air chamber (D), a watertight synthetic box (E), the aortic dissection model (F),a blood pressure cuff (G) an open reservoir (H).

90mmHg) and normocardia (60 beats per minute), parameters to simulate optimal hemodynamic parameters. The synthetic box was filled with water resulting in a submerged aortic dissection for optimal ultra-sound visualization.

## Imaging

Ultrasound **(**Zonare, Silicon Valley, California, USA**)** was used for imaging. The linear transducer (14 mHz) was used to visualize the transverse plane at four different locations in the model; the true lumen, the proximal false lumen, the mid false lumen and the distal false lumen (Figure 1).

Five cardiac cycles were recorded in the transverse plane at the four different locations in each model (Figure 1.). Anterior-posterior (AP) lumen diameter measurements were performed at baseline and after siliconizing. The maximal and minimal AP lumen diameter ($AP_{max,}$ $AP_{min}$) were identified as the ultra-sound image with the largest and smallest lumen diameter during cardiac cycle. In order to prevent inter observer variability, $AP_{max}$ and $AP_{min}$ measurements were performed by two different observers (HV and EP) blinded to the first outcome.

## Pressure measurements

Pressure measurements were performed in the center of the four different locations in the model; the true lumen (TL), the proximal false lumen (PFL), the mid false lumen (MFL) and the distal false

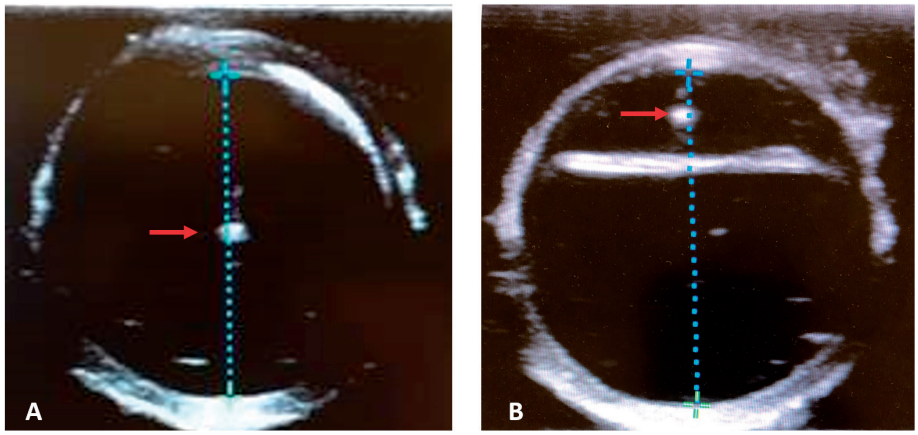


**Figure 3.** Ultrasound image of diameter and pressure measurement in the true (A) and false (B) lumen
**Red arrow:** the tip of the arterial catheter. Blue line: Anterior-Posterior (AP) lumen diameter.

lumen (DFL) (Figure 1). An arterial catheter (Patient Draeger Infinity Delta Monitor (Draeger, Inc. Telford, Pennsylvania, USA)) was used for pressure measurements. Pressure measurements in the TL were maintained stable at MAP 90mmHg by arterial catheter monitoring. The arterial catheter was visualized by ultra sound and positioned in the center of each location (Figure 3). After 10 seconds the pressure was recorded.

### Statistics

Lumen diameters $AP_{max}$, $AP_{min}$ and pressure measurements of the true and false lumen at all four locations in the aortic dissection planes were determined at baseline and after siliconizing. Mean values and standard deviations are reported. Paired t-tests were used to determine statistical significance in diameter and pressure change at each location in the aortic dissection model. Statistical significance was assumed at $p < 0.05$. To calculate the significance IBM SPSS Statistics version 24.0 (Armonk, NY, USA) was used.

## RESULTS

At baseline each model had the same morphology and dissection length, though the diameters and dissection width differed (Table 1).

**Table 1.** Characteristics of baseline and siliconized models

| | Model 1 | | Model 2 | | Model 3 | |
|---|---|---|---|---|---|---|
| | Baseline | Siliconized | Baseline | Siliconized | Baseline | Siliconized |
| **True lumen – prior to the dissection - (mm)** | 18.8±0.3 | 18.2±2.1 | 18.5±0.5 | 17.7±0.3 | 17.9±0.6 | 15.4±0.4 |
| ***P-value*** | *0.01* | | *0.01* | | *0.02* | |
| **True lumen reduction (%)** | 3.2 | | 4.1 | | 14.0 | |
| **MAP (mmHg)** | 90 | | 90 | | 90 | |
| **Total Proximal Lumen (mm)** | 19.5±1.3 | 18.1±0.8 | 18.9±1.5 | 17.8±1.6 | 17.1±0.5 | 15.1±1.5 |
| **Total Mid Lumen (mm)** | 18.5±0.6 | 17.4±2.2 | 18.6±2.4 | 17.2±2.8 | 16.1±1.0 | 14.8±0.8 |
| **Total Distal Lumen (mm)** | 17.8±1.0 | 17.0±0.3 | 17.7±0.6 | 16.3±1.1 | 15.7±0.6 | 14.1±1.4 |
| **Proximal True Lumen (PTL) (mm)** | 13.2±1.1 | 13.0±0.3 | 11.9±1.2 | 11.5±0.5 | 10.6±0.2 | 9.5±0.2 |
| **Mid True Lumen (MTL) (mm)** | 11.9±0.3 | 10.6±1.4 | 10.5±2.2 | 7.1±0.7 | 9.6±0.4 | 7.7±0.4 |
| **Distal True Lumen (DTL) (mm)** | 10.9±0.2 | 9.3±0.2 | 9.1±0.2 | 3.8±0.6 | 9.0±0.4 | 6.3±0.3 |
| **Proximal False Lumen (PFL) (mm)** | 6.3±0.2 | 5.1±0.5 | 7.0±0.3 | 6.1±1.1 | 6.5±0.3 | 5.6±1.3 |
| ***P-value*** | *0.07* | | *0.04* | | *0.08* | |
| **Proximal False Lumen (PFL) MAP (mmHg)** | 90±2.3 | 92±2.8 | 90±2.3 | 91±2.0 | 90±1.9 | 94±2.3 |
| ***P-value*** | *0.08* | | *0.36* | | *0.25* | |
| **Mid False Lumen (MFL) (mm)** | 6.6±0.3 | 6.8±0.8 | 8.1±0.2 | 10.1±2.1 | 6.5±0.6 | 7.1±0.4 |
| ***P-value*** | *0.01* | | *0.01* | | *0.03* | |
| **Mid False Lumen (MFL) MAP (mmHg)** | 90±1.4 | 92±1.8 | 90±0.6 | 91±2.1 | 91±2.6 | 95±3.2 |
| ***P-value*** | *0.9* | | *0.8* | | *0.6* | |
| **Distal False Lumen (DFL) (mm)** | 6.9±0.8 | 7.7±0.1 | 8.6±0.4 | 12.5±0.5 | 6.7±0.2 | 7.8±1.1 |
| ***P-value*** | *0.04* | | *<0.01* | | *0.03* | |
| **Distal False Lumen (DFL) MAP (mmHg)** | 91±2.2 | 92±1.3 | 90±1.5 | 92±1.3 | 91±0.6 | 95±3.2 |
| ***P-value*** | *0.9* | | *0.8* | | *0.8* | |

## True lumen (TL)

The aortic wall elasticity was decreased in all three models after siliconizing. Model 1 showed a mean true lumen reduction of 3.2%; 18.8 to 18.2 mm (md 18.5 ± 0.40 mm, *p=0.01*), model 2 a reduction of 4.1%; 18.5 to 17.7 mm (md 18.1 ± 0.50 mm, *p=0.01*) and model 3 showed a reduction of 14.0%; 17.9 to 15.4 mm (md 16.7 ± 1.77 mm, *p=0.05*).

The MAP in the TL was maintained stable at 90 mmHg.

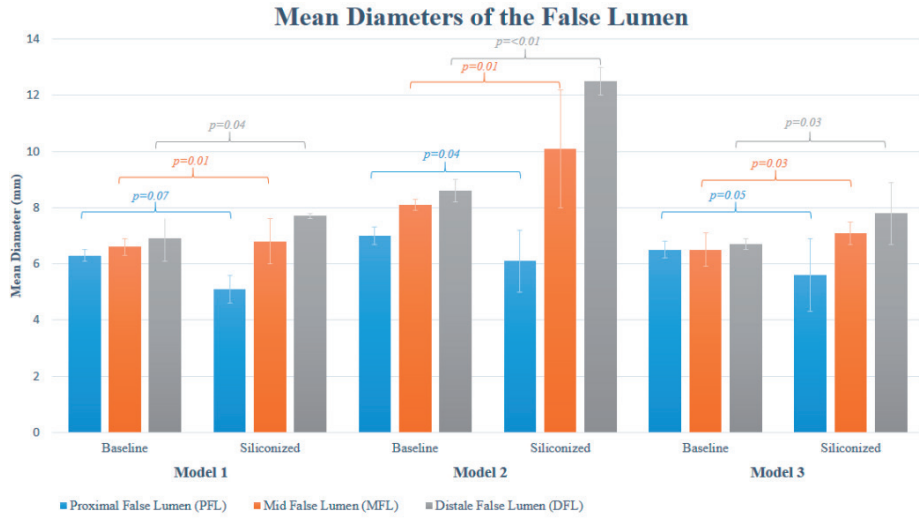


**Figure 4.** Mean diameters of the false lumen

### Proximal False lumen (PFL)

The PFL diameter only decreased significantly in model 2 after siliconizing. In model 1 and 3 there were no significant diameter changes. The MAP did not change significantly after siliconizing in all three models (Table 1).

### Mid and Distal False Lumen (MFL)

In all three siliconized models a significant increase of the MFL diameter was observed after siliconizing (Figure 4) although the MAP did not show statistically significant difference (Table 1).

## DISCUSSION

In this study the influence of aortic wall elasticity on the diameter and pressure of the false lumen in porcine aortic dissection models was evaluated. The main findings of this study are that an aortic wall with reduced elasticity results in an increased false lumen diameter in the mid and distal part of the false lumen.

Uncomplicated ABAD in the acute phase (0-2 weeks) are managed with surveillance and optimal medical treatment (OMT) with control of hypertension and heart rate.[1] When the uncomplicated ABAD converts to a complicated ABAD the mortality quadruples.[2] Gaining more insight in the false lumen behaviour of the uncomplicated ABAD mighty result in identifying those that are at high risk of developing complications. in the acute phase.

The majority of experimental flow studies in the field of aortic diseases are based on rigid wall models, under the assumption that the effect of wall elasticity on the quantitative results is rather limited for the haemodynamic parameters studied. These studies using mainly silicon tubing showed that lack of a distal tear results in a significant increase in diastolic pressure presumably due to an impairment of outflow from the false lumen to the true lumen.[7] Increased pressure of the false lumen results in increased wall stress of the false lumen.[8] This may contribute to a progression of the dissection and convert an uncomplicated into a complicated dissection. However, besides hemodynamic changes and dissection morphology, aortic wall elasticity may have a major influence on the course of the false lumen.

Currently, there is one published article that compares pressure in the false lumen with a changing elasticity of the aorta wall.[12] However, synthetic polymer of silicon tubing was used in their in-vitro study. No further studies have examined the unique effect of wall elasticity on the false lumen, independent of other parameters. An in-vitro study in the previously validated aortic dissection model has the potential to study a specific parameter in a controlled setting.[14,17] In this study, a porcine aorta – instead of synthetic polymer or silicon tubing - was used as a 'modeled' aorta.[7,18] Research showed that elasticity and morphology of a young porcine aorta corresponds to the human thoracic aorta under 65 years.[19] In addition, the morphology of a surgically created false lumen in a porcine aorta dissection is comparable to a human aortic dissection.[13] In this study the baseline models mimic the thoracic aorta under 65 years, where the siliconized model mimics the more rigid (atherosclerotic) thoracic aorta. This study and our previous studies showed that this ex-vivo porcine model is a representative model to study different aspects of ABAD.[14,17] In all three models the aortic wall elasticity (expressed in AP diameter change) was significantly decreased after siliconizing. The diameter of the MFL and DFL expanded significantly in all models when the aortic wall elasticity decreased. The MAP did not significantly change in the MFL and DFL in all three models. The observed increase in false lumen diameter of the MFL and DFL can be explained by the fact that the dissection flap is thinner than the (partial thickness media with adventitia) outer aortic wall. When the outer aortic wall stiffness disproportionate increases compared to the dissection flap stiffness, the dissection flap will be pushed further away from the outer aortic wall, resulting in an increase in the false lumen diameter.

The presented in-vitro model has limitations. First, we used water instead of blood as a circulating fluid, which has a much lower viscosity than blood. However, in our experimental setup blood cannot be used because of the thrombotic effect which will affect the tubing system or pulsatile pump.[13] Secondly, the aortas were defrosted, prepared and thawed within 1 day, which could have affected the elasticity of the aortic wall at baseline. Furthermore, the diameter of a porcine aorta is smaller than that of humans. Still, this study demonstrates that wall elasticity is clearly altering the false lumen and should be taken into account when assessing and studying aortic dissections. With the rapid development of new MRI technology for vessel wall imaging wall elasticity can be determined although translation of the results of this study to a physiological situation is limited and evaluation of patients should be performed to confirm our findings.

In conclusion, this in-vitro study showed that an aortic wall with reduced elasticity of the outer aortic layers results in an increased false lumen diameter in the mid and distal part of the false lumen. False lumen expansion might result in higher stress of the aortic wall and at the ending of the dissection. The present model provides information on the role of the elasticity of the outer aortic layers in the context of experimental aortic dissection, but that the results can certainly only be transferred to corresponding clinical situations to a limited extent.

## REFERENCE LIST


1. Tolenaar JL, Van bogerijen GH, Eagle KA, Trimarchi S. Update in the management of aortic dissection. Curr Treat Options Cardiovasc Med. 2013;15(2):200-13.
2. Brunkwall J, Kasprzak P, Verhoeven E, et al. Endovascular repair of acute uncomplicated aortic type B dissection promotes aortic remodelling: 1 year results of the ADSORB trial. Eur J Vasc Endovasc Surg. 2014;48(3):285-91.
3. Nienaber CA, Kische S, Rousseau H, et al. Endovascular repair of type B aortic dissection: long-term results of the randomized investigation of stent grafts in aortic dissection trial. Circ Cardiovasc Interv. 2013;6(4):407-16.
4. Yuan X, Mitsis A, Ghonem M, Iakovakis I, Nienaber CA. Conservative management versus endovascular or open surgery in the spectrum of type B aortic dissection. J Vis Surg. 2018;4:59.
5. DeBakey ME, Henly WS, Cooley DA, et al. Surgical management of dissecting aneurysms of the aorta. J Thorac Cardiovasc Surg. 1965;49:130–149.
6. Rudenick PA, Segers P, Pineda V, et al. False Lumen Flow Patterns and their Relation with Morphological and Biomechanical Characteristics of Chronic Aortic Dissections. Computational Model Compared with Magnetic Resonance Imaging Measurements. PLoS ONE. 2017;12(1):e0170888.
7. Tsai TT, Schlicht MS, Khanafer K, et al. Tear size and location impacts false lumen pressure in an ex vivo model of chronic type B aortic dissection. J Vasc Surg. 2008;47(4):844-51.
8. Veger HTC, Pasveer EH, Wever JJ, et al. Wall shear stress assessment of the false lumen in abad visualized by 4D flow MRI. J Cardiovasc Surg, abstract book. 2019;60(1):10.
9. Nienaber CA, Eagle KA. Aortic dissection: new frontiers in diagnosis and management: Part II: therapeutic management and follow-up. Circulation. 2003;108(6):772-8.
10. Wu D, Shen YH, Russell L, Coselli JS, Lemaire SA. Molecular mechanisms of thoracic aortic dissection. J Surg Res. 2013;184(2):907-24.
11. Ageing and Vascular Ageing. Jani B, Rajkumar C. Postgrad Med J. 2006 Jun;82(968):357-62.
12. Rudenick PA, Bijnens BH, Segers P, García-dorado D, Evangelista A. Assessment of wall elasticity variations on intraluminal haemodynamics in descending aortic dissections using a lumped-parameter model. PLoS ONE. 2015;10(4):e0124011.
13. Qing KX, Chan YC, Lau SF, Yiu WK, Ting AC, Cheng SW. Ex-vivo haemodynamic models for the study of Stanford type B aortic dissection in isolated porcine aorta. Eur J Vasc Endovasc Surg. 2012;44(4):399-405.
14. Veger HT, Westenberg JJ, Visser MJ. The role of branch vessels in aortic type B dissection: an in vitro study. Eur J Vasc Endovasc Surg. 2015;49(4):375-81.
15. Bosman WM, Vlot J, Van der steenhoven TJ, et al. Aortic Customize: an in vivo feasibility study of a percutaneous technique for the repair of aortic aneurysms using injectable elastomer. Eur J Vasc Endovasc Surg. 2010;40(1):65-70.
16. Hinnen JW, Rixen DJ, Koning OH, Van bockel HJ, Hamming JF. Aneurysm sac pressure monitoring: does the direction of pressure measurement matter in fibrinous thrombus?. J Vasc Surg. 2007;45(4):812-6.
17. Veger HTC, Pasveer EH, Visser MJT. Where to Fenestrate in Aortic Dissection Type B? An Ex Vivo Study. Ann Vasc Surg. 2017;43:296-301.
18. Chung JW, Elkins C, Sakai T, et al. True-lumen collapse in aortic dissection: part II. Evaluation of treatment methods in phantoms with pulsatile flow. Radiology. 2000;214(1):99-106.
19. De beaufort HWL, Ferrara A, Conti M, et al. Comparative Analysis of Porcine and Human Thoracic Aortic Stiffness. Eur J Vasc Endovasc Surg. 2018;55(4):560-566.

# 4

# Wall Shear Stress Assessment of the False Lumen in Acute Type B Aortic Dissection Visualized by Four-Dimensional Flow Magnetic Resonance Imaging (4D flow MRI) An ex-vivo study.

H.T.C. Veger
E.H. Pasveer
J.J. Wever
J.J.M. Westenberg
R.G. Statius van Eps

Vascular and Endovascular Surgery. 2021

## ABSTRACT

### Background

Four-dimensional flow magnetic resonance imaging **(**4D flow MRI) can visualize and quantify flow and provide hemodynamic information such as wall shear stress (WSS). More insight in the hemodynamic changes during cardiac cycle in the true and false lumen of uncomplicated acute type B aortic dissection (ABAD) might result in prediction of adverse outcomes.

### Methods

A porcine aorta dissection model with an artificial dissection was positioned in a validated ex-vivo circulatory system with physiological pulsatile flow. 4D flow MR images with three set heartrates (HR; 60, 80 and 100 bpm) were acquired. False lumen volume per cycle (FLV), mean and peak systolic WSS were determined from 4D flow MRI data. For validation, the experiment was repeated with a second porcine aorta dissection model.

### Results

During both experiments an increase in FLV (initial experiment: ΔFLV = 2.05 ml, $p<0.001$, repeated experiment: ΔFLV = 1.08 ml, $p=0.005$) and peak WSS (initial experiment: ΔWSS = 1.2 Pa, $p=0.004$, repeated experiment: ΔWSS = 1.79 Pa, $p=0.016$) was observed when HR increased from 60 to 80 bpm. Raising the HR from 80 to 100 bpm, no significant increase in FLV ($p=0.073$, $p=0.139$) was seen during both experiments. The false lumen mean peak WSS increased significant during initial (2.71 to 3.85 Pa; $p=0.013$) and non-significant during repeated experiment (3.22 to 4.00 Pa; $p=0.320$)

### Conclusion

Our experiments showed that an increase in HR from 60 to 80 bpm resulted in a significant increase of FLV and WSS of the false lumen. We suggest that strict heart rate control is of major importance to reduce the mean and peak WSS in uncomplicated ABAD. Because of limitations of an ex-vivo study, 4D flow MRI will have to be performed in clinical setting to determine whether this imaging model would be of value to predict the course of uncomplicated ABAD.

## INTRODUCTION

An uncomplicated Acute Type B Aortic Dissection (ABAD) will worsen into a complicated ABAD in approximately 20-30% of cases.[1-3] Once complications occur the prognosis of ABAD dramatically declines to 30 days hospital mortality of over 10%. [1,2,4] Guidelines are well established regarding complicated ABAD and there are no controversies regarding the need to treat them with TEVAR.[5] On the contrary, the uncomplicated acute type B aortic dissections are prone to discussion.[3] Uncomplicated ABAD has a relatively poor prognosis. The reason for this is due to the heterogeneity of the disease and unpredictable course.[6] Identification of clinical and imaging predictors of adverse outcomes in uncomplicated ABAD seems mandatory in order to identify those patients who will benefit from early intervention by TEVAR.[7]

The gold standard for imaging ABAD is Computed Tomography Angiography (CTA).[8] However, because of the static aspect of CTA images, interpretation of the volume and flow changes in the true and false lumen during cardiac cycle is not possible. To get more insight in these hemodynamic changes Four-dimensional flow magnetic resonance imaging (4D flow MRI) might be helpful.[9] This imaging technique can accurately visualize and quantify flow and provide hemodynamic information such as wall shear stress (WSS).[10-12] In arterial blood flow, the WSS expresses the viscous force per unit area applied by the fluid on the wall in a direction at the local interface.[13] Gaining more insight of these forces in the true but especially the false lumen in uncomplicated ABAD during optimal medical treatment, might result in prediction of adverse outcomes. Several ex-vivo and in-vivo studies simulating chronic type B aortic dissection (CBAD) showed an increase in false lumen pressure during the longer diastolic phase resulting in increased wall tension over a longer period of the cardiac cycle.[14,15] These studies clearly showed how changes in heart rate can affect lumen pressure in CBAD. However, it can be argued that these ex- and in-vitro results in a CBAD model cannot be translated to dissection in the acute setting due to difference in dissection flap stiffness between ABAD and CBAD. The dissection flap changes during the transition from the acute to the chronic stage with an observed increase of dissection flap thickness over time.[16 17] In ABAD there might be more expansion of the false lumen resulting in higher wall shear stress (WSS) compared to CBAD. However, this has not been examined before in a validated ABAD model. Therefore, the purpose of this study was to examine the influence of heart rate (HR) on the volume, mean and peak WSS by 4D flow MRI in the false lumen in a validated ex-vivo porcine aorta dissection model inserted in a pulsatile flow-model simulating uncomplicated ABAD.

We hypothesized that HR, volume and WSS have a linear correlation within the false lumen of patients with uncomplicated ABAD.

## MATERIALS AND METHODS

### Aortic dissection model

Frozen unmodified porcine aortas were obtained from the abattoir. They were thawed and prepared as follows: from the aortic arch to the iliac bifurcation all side branches were ligated with 5.0 Prolene. The aorta was inverted inside out and the wall was punctured by a needle. Injection of water resulted in a dissection and the dissection flap was cut in a proximal location to create a primary entry. This technique was previously described by Qing et al.[18]

The created false lumen in the media depicts an anatomic situation comparable to an acute human aortic dissection.[7] In order to study reproducibility, the experiment was repeated with another porcine aorta with a similar morphology. Institutional Review Board (IRB) approval was not needed because no animals were sacrificed specifically for this study.

### In-vitro circulatory system

A validated in-vitro circulatory system with physiological flow and pressure characteristics was used to mimic the human circulatory system.[7,19,20] The main components of this circulatory system are a pneumatically-driven pulsatile pump, a compliance chamber and the watertight synthetic box with the aortic dissection model (Figure 1).[7] All components are connected by a silicone tubing

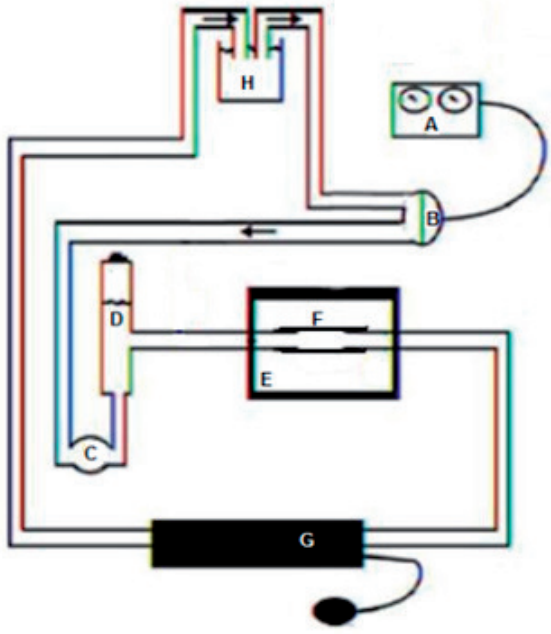


**Figure 1.** Circulation set-up. A schematic representation of the circulation set-up, which consisted of an artificial heart driver (A), left ventricle (B), a ball valve (C), an air chamber (D), a watertight synthetic box (E), the aortic dissection model (F),a blood pressure cuff (G) an open reservoir (H).

system and water was used for circulating fluid.[7] The synthetic box with the aortic dissection model was placed inside the MRI gantry. Before MRI-scanning started, blood pressure was set to 120/80 mmHg. Both models were imaged at a HR of 60 bpm, 80 bpm and 100 bpm. An arterial catheter (Patient Draeger Infinity Delta Monitor (Drager, Inc. Telford, Pennsylvania, USA)) was used to keep the blood pressure at 120/80 mmHg during the experiments.

### Imaging

3D Time resolved MRI imaging with velocity encoding in three directions was performed to obtain 4D Flow MRI data. Imaging was performed on a *1.5T* MRI system (Ingenia; Philips Healthcare, Best, the Netherlands).

For each 4D Flow MRI acquisition, 35 phases were retrospectively reconstructed. The acquired spatial resolution in the MRI protocol was 1 × 2 × 2 $mm^3$. Specific imaging parameters were as follows: echo time 4.2 ms, repetition time 7.9 ms, flip angle 10°, slice thickness 2 mm, field-of-view 133 × 300 $mm^2$, matrix size 133×152 and velocity encoding with sensitivity of 100 or 120 cm/s. Acceleration was achieved by Echo Planar Imaging to factor of 5.

Image analysis was performed using in-house developed and validated MASS software using manual contour segmentation.[21] In order to obtain the false lumen volume (FLV), the dissection segment was divided into three equal parts, the proximal, mid and distal part. Subsequently, the lumen region of both true and false lumen was manually segmented for all three parts separately and at each phase of the cardiac cycle for a total of 40 phases. True and false lumen area (in $mm^2$) versus time graphs were defined. After segmentation, an average false lumen was obtained.

To calculate the WSS CAAS MR Solutions software v5.0 (Pie Medical Imaging, Maastricht, The Netherlands) was used. Both models were manually segmented at each HR for five phases (two before and two after peak systole) separately. The segmented WSS was then determined for each phase. For each phase a mean and peak segmented WSS was calculated. Thereafter the mean of the five phases was used to measure the difference between two HR's for each model.

### Statistics

To calculate the data IBM SPSS Statistics version 24.0 (Armonk, NY) was used. Mean values and standard deviations are reported. A paired t-test was used to compare the mean between two separate HR's within the same model. A p-value $<0.05$ was considered significant.

## RESULTS

### Heart rate increase from 60 to 80 bpm

The FLV increased significant during the initial (13.3 to 15.3 ml; $p<0.001$) and repeated experiment (12.8 to 13.9 ml; $p=0.005$). The TLV decreased during the initial experiment but slightly increased in the repeated experiment (19.7 to 17.0ml; $p<0.001$). The false lumen mean WSS increased

significant during initial (0.44 to 0.63 Pa; *p=0.007*) and repeated experiment (0.31 to 0.56 Pa; *p=0.009*) (Table 1.; Figures 3 and 4.). The false lumen mean peak WSS increased significant during initial (1.51 to 2.71 Pa; *p=0.004*) and repeated experiment (1.43 to 3.22 Pa; *p=0.016*) (Table 1.; Figures 3 and 4.).

**Table 1.** Results FLV and WSS

| | Initial experiment | | | Repeated experiment | | |
|---|---|---|---|---|---|---|
| **Heart rate (bpm)** | 60 | 80* | 100 | 60 | 80 | 100 |
| **RR (mmHg)** | 120/80 | 120/80 | 120/80 | 120/80 | 120/80 | 120/80 |
| **True lumen volume (ml)** | 19.7±0.05 | 17.0±0.01 | 16.9±0.03 | 18.5±0.07 | 18.8±0.02 | 18.8±0.03 |
| *p-value* | <0.001 | 0.250 | | 0.010 | 0.742 | |
| **False lumen volume (ml)** | 13.3±0.02 | 15.3±0.02 | 15.3±0.04 | 12.83±0.11 | 13.9±0.02 | 13.7±0.11 |
| *p-value* | <0.001 | 0.073 | | 0.005 | 0.139 | |
| **False lumen WSS (Pa)** | 0.462 | 0.728 | 0.383 | 0.306 | 0.565 | 0.601 |
| | 0.431 | 0.608 | 0.493 | 0.317 | 0.448 | 0.645 |
| | 0.430 | 0.660 | 0.474 | 0.327 | 0.625 | 0.734 |
| | 0.438 | 0.492 | 0.463 | 0.353 | # | 0.572 |
| | 0.447 | 0.666 | 0.393 | 0.302 | 0.617 | 0.612 |
| **False lumen mean WSS (Pa)** | 0.44 ± 0.01 | 0.63 ± 0.09 | 0.44 ± 0.05 | 0.31 ± 0.01 | 0.56 ± 0.08 | 0.65 ± 0.06 |
| *p-value* | 0.007 | 0.027 | | 0.009 | 0.154 | |
| **False lumen Peak WSS (Pa)** | 1.487 | 2.548 | 3.312 | 1.288 | 3.673 | 3.132 |
| | 1.650 | 2.510 | 3.858 | 1.374 | 2.117 | 3.462 |
| | 1.553 | 2.559 | 4.648 | 1.496 | 3.407 | 5.763 |
| | 1.463 | 3.460 | 4.100 | 1.656 | # | 2.744 |
| | 1.390 | 2.488 | 3.326 | 1.565 | 3.684 | 3.653 |
| **False lumen Mean Peak WSS (Pa)** | 1.51 ± 0.10 | 2.71 ± 0.42 | 3.85 ± 0.56 | 1.43 ± 0.12 | 3.22 ± 0.75 | 4.00 ± 1.19 |
| *p-value* | 0.004 | 0.013 | | 0.016 | 0.320 | |

* See Figure 2. for illustration.

# CAAS did not allow to access five phases for model 2 with HR 80 bpm, therefore in this case, only 4 phases were available.

## Heart rate increase from 80 to 100 bpm

There was no significant change neither in FLV during the initial (15.3 to 15.3 ml; *p=0.07*) and repeated experiment (13.9 to 13.7 ml; *p=0.139*) nor in TLV during the initial (17.0 to 16.9 ml; *p=0.25*) and repeated experiment (18.8 to 18.8 ml; *p=0.74*). The false lumen mean WSS decreased significant during initial experiment (0.63 to 0.44 Pa; *p=0.027*) but increased significant during repeated experiment (0.56 to 0.65 Pa; *p=0.154*) (Table 1.; Figures 3 and 4.). The false lumen mean

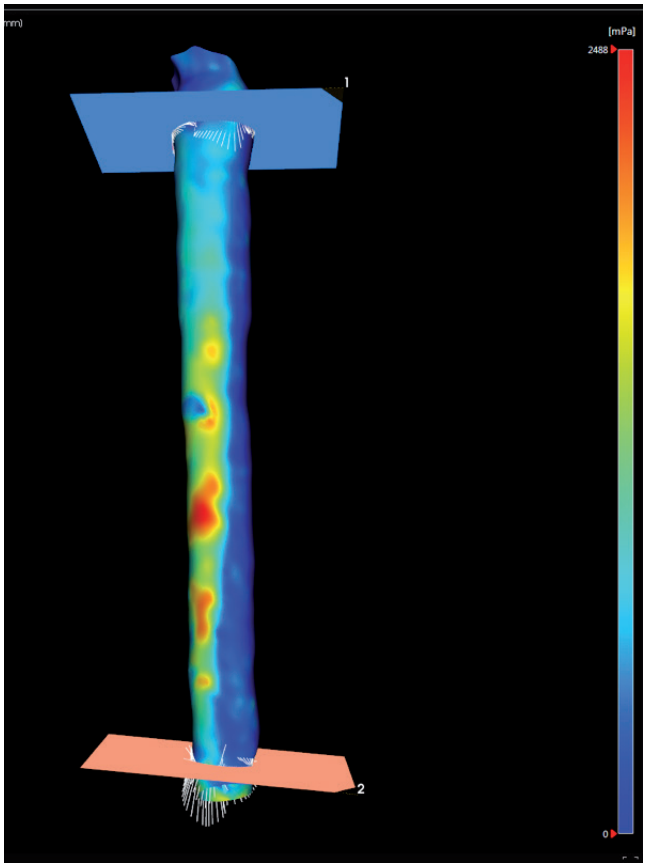


**Figure 2.** 4D MRI image of initial experiment at a HR of 80 bpm. A map of WSS based on 4D MR images (blue = low WSS, red = high WSS).

peak WSS increased significant during initial (2.71 to 3.85 Pa; *p=0.013*) and non-significant during repeated experiment (3.22 to 4.00 Pa; *p=0.320*) (Table 1.; Figures 3 and 4.).

## DISCUSSION

Still today it is difficult to predict the clinical course of uncomplicated ABAD. The optimum management of patients with uncomplicated ABAD is unclear.[3] The principal management of ABAD remains aggressive medical therapy for all patients, with TEVAR primarily reserved for those who develop complications.[3] In order to gain more understanding in uncomplicated ABAD it might be helpful to clarify the hemodynamic changes during the cardiac cycle with 4D flow MRI.[9]

4D flow MRI can accurately visualize and quantify the functional flow and access hemodynamic information such as WSS.[10,11] During a recent in-vivo scan-rescan study by van der Palen et al, the

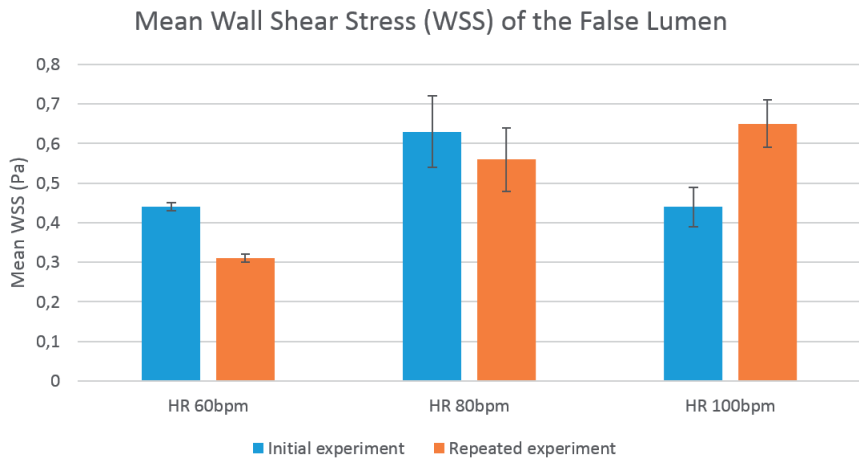


**Figure 3.** Mean Wall Shear Stress (WSS) of the False Lumen during both experiments

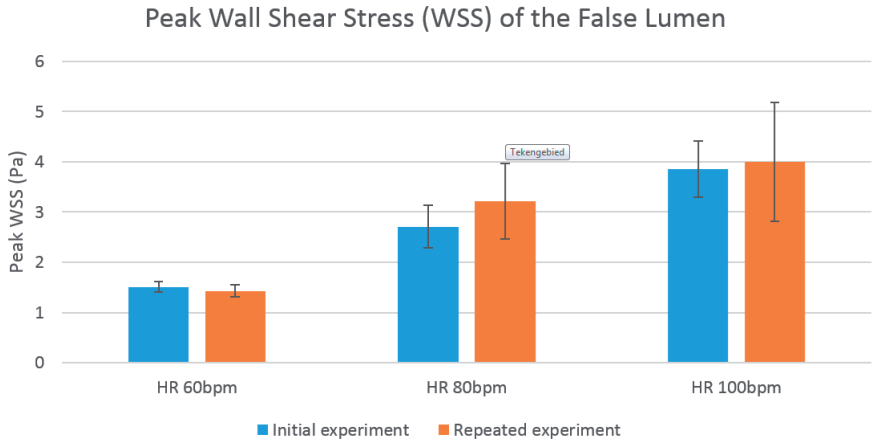


**Figure 4.** Peak Wall Shear Stress (WSS) of the False Lumen during both experiments

reproducibility of segmental aortic 3D systolic WSS by phase-specific segmentation with 4D flow MRI was evaluated and showed a very accurate reproducibility of the WSS assesments. During our study the same tools, with respect to 4D flow MRI acquisition and analysis were used.[12]

The presented porcine aortic dissection models simulate ABAD, as the morphology of a surgically created false lumen in a porcine aorta dissection is comparable to a human aortic dissection and the dissection flaps are soft.[16] Furthermore, de Beaufort et al. showed that morphology and elasticity of young porcine aortas corresponds to the human thoracic aortic under 65 years.[22] This implies together with our previously published studies that our ex-vivo porcine aorta model is a representative model to study uncomplicated ABAD.[7,23] Earlier research on aortic dissection by 4D flow MRI was only performed using silicon models and resulted in hemodynamic insights into

aortic dissection.[4] Other in-vitro study on hemodynamics in aorta dissection showed that if a distal tear in the false lumen was absent the diastolic pressure in the false lumen increased compared to the true lumen diastolic pressure.[14] However, it should be noted that these last two mentioned studies did not use biological tissue but were based on experiments with synthetic polymer or silicon tubing.[4,14,24] Data from these studies were intended to mimic a chronic dissection model. The set-up of our study by using an ex-vivo porcine aorta model is more representative to simulate ABAD.

This study showed a significant increase in FLV, mean WSS and peak WSS during the initial and repeated experiment when HR raised from 60 to 80 bpm. These results support the recommendations of goal-directed therapy to establish and control a heart rate of less than 60 bpm in the 2010 ACCF/AHA/AATS/ACR/ASA/SCA/SCAI/SIR/STS/SVM Guidelines for the Diagnosis and Management of Patients With Thoracic Aortic Disease.[25] Interestingly, when the HR raised from 80 to 100 bpm, no significant increase in FLV was observed but increase of mean and peak WSS were measured (Table 1, Figures 3 and 4). This finding indicates that a stable FLV does not exclude an increase in mean and peak WSS. It illustrates the added value of 4D MRI, in gaining additional hemodynamic information compared to conventional imaging modalities. Our hypothesis that HR and WSS have a linear correlation within the false lumen of uncomplicated ABAD could only be proved statistically in our ex-vivo porcine aorta dissection model when HR raised from 60 to 80 bpm.

Our study has several limitations being an experimental ex-vivo model. Firstly the porcine aorta models during the initial and repeated experiment have the same morphology but there are mild differences (Table 1.). These might be responsible for the observed differences between the initial and repeated experiment. Secondly, the diameter of a porcine aortic is smaller than that of humans. Thirdly, the viscosity of water is much lower than that of blood which might have its influence on the wall shear stress. However, blood could not be used in our set-up because of a risk of thrombosis, which can block the tubing system or the pulsatile pump.[16] Lastly, the porcine aorta in our model was no longer surrounded by connective tissue that also affects aorta compliance.

In conclusion, 4D flow MRI compared to CTA provides insight into hemodynamic dimensions such as WSS. This information might result in better understanding of the false and true lumen behavior in uncomplicated ABAD at presentation and might provide the opportunity to better predict the clinical course of this disease. Our ex-vivo research illustrated that an increase in HR from 60 to 80 bpm resulted in a significantly increase of the FLV and WSS of the false lumen. We suggest that strict heart rate control is of major importance to reduce the mean and peak WSS in uncomplicated ABAD. Because of the limitations of an ex-vivo study, 4D flow MRI will have to be performed in clinical setting to determine whether this imaging model would be of value to predict the course of uncomplicated ABAD.

## REFERENCE LIST


(1) Yuan X, Mitsis A, Ghonem M, Iakovakis I, Nienaber CA. Conservative management versus endovascular or open surgery in the spectrum of type B aortic dissection. J Vis Surg. 2018;4:59.

(2) Moulakakis KG, Mylonas SN, Dalainas I, Kakisis J, Kotsis T, Liapis CD. Management of complicated and uncomplicated acute type B dissection. A systematic review and meta-analysis. Ann Cardiothorac Surg. 2014;3(3):234-46.

(3) Scott AJ, Bicknell CD. Contemporary Management of Acute Type B Dissection. Eur J Vasc Endovasc Surg. 2016;51(3):452-9.

(4) Birjiniuk J, Timmins LH, Young M, et al. Pulsatile Flow Leads to Intimal Flap Motion and Flow Reversal in an In Vitro Model of Type B Aortic Dissection. Cardiovasc Eng Technol. 2017;8(3):378-389.

(5) Schermerhorn ML, Jones DW. Management of Descending Thoracic Aorta Disease: Evolving Treatment Paradigms in the TEVAR Era. Eur J Vasc Endovasc Surg. 2017;53(1):1-3.

(6) Birjiniuk J, Ruddy JM, Iffrig E, et al. Development and testing of a silicone in vitro model of descending aortic dissection. J Surg Res. 2015;198(2):502-7

(7) Veger HT, Westenberg JJ, Visser MJ. The role of branch vessels in aortic type B dissection: an in vitro study. Eur J Vasc Endovasc Surg. 2015;49(4):375-81.

(8) Khayat M, Cooper KJ, Khaja MS, Gandhi R, Bryce YC, Williams DM. Endovascular management of acute aortic dissection. Cardiovasc Diagn Ther. 2018;8(Suppl 1):S97-S107.

(9) François CJ, Markl M, Schiebler ML, et al. Four-dimensional, flow-sensitive magnetic resonance imaging of blood flow patterns in thoracic aortic dissections. J Thorac Cardiovasc Surg. 2013;145(5):1359-66.

(10) Kinner S, Eggebrecht H, Maderwald S, et al. Dynamic MR angiography in acute aortic dissection. J Magn Reson Imaging. 2015;42(2):505-14.

(11) Clough RE, Waltham M, Giese D, Taylor PR, Schaeffter T. A new imaging method for assessment of aortic dissection using four-dimensional phase contrast magnetic resonance imaging. J Vasc Surg. 2012;55(4):914-23.

(12) Van der palen RLF, Roest AAW, Van den boogaard PJ, De roos A, Blom NA, Westenberg JJM. Scan-rescan reproducibility of segmental aortic wall shear stress as assessed by phase-specific segmentation with 4D flow MRI in healthy volunteers. MAGMA. 2018;31(5):653-663.

(13) Katritsis D, Kaiktsis L, Chaniotis A, Pantos J, Efstathopoulos EP, Marmarelis V. Wall shear stress: theoretical considerations and methods of measurement. Prog Cardiovasc Dis. 2007;49(5):307-29.

(14) Tsai TT, Schlicht MS, Khanafer K, et al. Tear size and location impacts false lumen pressure in an ex vivo model of chronic type B aortic dissection. J Vasc Surg. 2008;47(4):844-51.

(15) Rudenick PA, Bijnens BH, García-dorado D, Evangelista A. An in vitro phantom study on the influence of tear size and configuration on the hemodynamics of the lumina in chronic type B aortic dissections. J Vasc Surg. 2013;57(2):464-474.e5.

(16) Peterss S, Mansour AM, Ross JA, Vaitkeviciute I, Charilaou P, Dumfarth J, Fang H, Ziganshin BA, Rizzo JA, Adeniran AJ, Elefteriades JA. Changing Pathology of the Thoracic Aorta From Acute to Chronic Dissection: Literature Review and Insights. J Am Coll Cardiol. 2016 Sep 6;68(10):1054-65. doi: 10.1016/j.jacc.2016.05.091.

(17) Karmonik C, Duran C, Shah DJ, Anaya-Ayala JE, Davies MG, Lumsden AB, Bismuth J. Preliminary findings in quantification of changes in septal motion during follow-up of type B aortic dissections. J Vasc Surg. 2012 May;55(5):1419-26. doi: 10.1016/j.jvs.2011.10.127.

(18) Qing KX, Chan YC, Lau SF, Yiu WK, Ting AC, Cheng SW. Ex-vivo haemodynamic models for the study of Stanford type B aortic dissection in isolated porcine aorta. Eur J Vasc Endovasc Surg. 2012;44(4):399-405.

(19) Bosman WM, Vlot J, Van der steenhoven TJ, et al. Aortic Customize: an in vivo feasibility study of a percutaneous technique for the repair of aortic aneurysms using injectable elastomer. Eur J Vasc Endovasc Surg. 2010;40(1):65-70.

(20) Hinnen JW, Rixen DJ, Koning OH, Van bockel HJ, Hamming JF. Aneurysm sac pressure monitoring: does the direction of pressure measurement matter in fibrinous thrombus?. J Vasc Surg. 2007;45(4):812-6.

(21) Van der geest RJ, Reiber JH. Quantification in cardiac MRI. J Magn Reson Imaging. 1999;10(5):602-8.

(22) De beaufort HWL, Ferrara A, Conti M, et al. Comparative Analysis of Porcine and Human Thoracic Aortic Stiffness. Eur J Vasc Endovasc Surg. 2018;55(4):560-566.

(23) Veger HTC, Pasveer EH, Visser MJT. Where to Fenestrate in Aortic Dissection Type B? An Ex Vivo Study. Ann Vasc Surg. 2017;43:296-301.

(24) Chung JW, Elkins C, Sakai T, et al. True-lumen collapse in aortic dissection: part II. Evaluation of treatment methods in phantoms with pulsatile flow. Radiology. 2000;214(1):99-106.

(25) Hiratzka LF, Bakris GL, Beckman JA, et al. 2010 ACCF/AHA/AATS/ACR/ASA/SCA/SCAI/SIR/STS/SVM guidelines for the diagnosis and management of patients with Thoracic Aortic Disease: a report of the American College of Cardiology Foundation/American Heart Association Task Force on Practice Guidelines, American Association for Thoracic Surgery, American College of Radiology, American Stroke Association, Society of Cardiovascular Anesthesiologists, Society for Cardiovascular Angiography and Interventions, Society of Interventional Radiology, Society of Thoracic Surgeons, and Society for Vascular Medicine. Circulation. 2010;121(13):e266-369.

# 5

# Where to Fenestrate in Type B Aortic Dissection? An ex-vivo study.

H.T.C. Veger
E.H. Pasveer
M.J.T. Visser

*Annals of Vascular Surgery. 2017*

## ABSTRACT

### Purpose

Fenestration is a minimally invasive alternative for the treatment of acute symptomatic aortic dissections because it may quickly decrease the pressure gradient of the false lumen. It remains unclear where the optimal location of these fenestrations should be chosen. The purpose of this study was to study false lumen volume after different fenestration strategies in porcine ex-vivo models of aortic type B dissection.

### Materials and Methods

An artificial dissection was created in ex-vivo porcine aortas. A total number of six aortic dissection models were made. The dissection flap was divided in three equal parts; proximal, mid and distal sections. In three models a fenestration was made in the center of the proximal section of the dissection flap. In the three others in the center of the distal part of the dissection flap. The aorta was positioned in a validated in vitro circulatory system with physiological pulsatile flow. Volume-measurements of true lumen volume (TLV) and false lumen volume (FLV) were assessed with computed tomography.

### Results

Performing a fenestration in the proximal part of the dissection flap resulted in FLV increase in two of the three models. Performing a fenestration in the distal part of the dissection flap resulted in FLV decrease in all three models. False lumen reduction was obtained significantly in the distally fenestrated models compared to the proximally fenestrated models (9.6±3.5% vs. 0.7±2.9%, $p=0.02$)

### Conclusion

In this in-vitro study, we showed that distal fenestration of the false lumen in aortic dissection will result in the largest false lumen reduction.

## INTRODUCTION

Acute type B Aortic Dissection (ABAD) is still today a catastrophic disorder. Visceral, renal, spinal and iliac malperfusion occurs in up to 30% of patients with ABAD and is strongly associated with worse outcome.[1] Malperfusion can be classified as dynamic or static.[1] Dynamic obstruction is caused by the prolapse of the dissection flap into the vessel ostium. The obstruction is usually evident during the aortic systole and causes about 80% of malperfusion syndromes. Static obstruction is the result of branch vessel compression by extension of the dissection flap into the branch and is present throughout the cardiac cycle. [1] Endovascular interventions in patients with ABAD include proximal entry closure by means of stent-graft implantation, bare metal stent implantation in the true aortic lumen or aortic branch vessels, and percutaneous balloon fenestration of the dissection flap.[2] The first line therapy in acute type B dissection with malperfusion syndrome is currently coverage of the proximal entry tear by Thoracic Endo-Vascular Aortic Repair (TEVAR).[1] When this method is unfeasible, endovascular aortic fenestration has been proposed as an alternative technique.[3] Endovascular aortic fenestration quickly decrease the pressure gradient of the false lumen and can also be an adjunctive tool to other endovascular interventions.[1 3 4 5] The most common endovascular technique to achieve a fenestration is the creation of a communicating hole between the false and the true lumen followed by balloon-dilatation.[5 6 7 8] Balloon-dilatation can be performed at one or multiple sites along the dissection membrane to achieve equalibration of pressures between the true and false lumens.[9] It remains unclear where the optimal location of these fenestrations should be made.[7] So, fenestration at optimal locations would result in acute depressurization of the false lumen with reduction of its volume as result. The objective was to study false lumen volume after different fenestration strategies in porcine ex-vivo models of aortic type B dissection. The impact of the fenestration-site comparing more proximal and distal locations was explored to study the hypothesis.

We hypothesize that a more distal location of the fenestration in the false lumen would lead to better equilibration of pressures and false lumen reduction. We performed two different fenestrations strategies in a validated ex-vivo porcine aorta dissection model in a pulsatile flow-model.[10] Computed tomography angiography was used for imaging and volume-measurements.

## MATERIALS AND METHODS

### Aortic dissection model

Unmodified porcine aortas were obtained frozen from the abattoir. They were defrozen and prepared as follows: from the aortic arch to the iliac bifurcation all side branches were ligated with 5.0 Prolene. The aorta was inverted inside out and the intima was punctured by a needle. Injection of water resulted in a dissection and the dissection flap was cut in a proximal location to create a primary entry. This technique was previously described by Qing et al.[11]

**Figure. 1.** (A) A turned over porcine aorta with an artificially created dissection. The fenestration in the dissection flap was made by a 10 x 40-mm Percutaneous Transluminal Angioplasty (PTA) balloon (Abbott Vascular, CA). (B) The fenestration in the dissection flap after removal of the PTA balloon is shown.

A total of six aortic dissection models were made. The dissection flap was longitudinally divided in three equal sections; proximal, mid and distal. In three models a fenestration was made in the center of the proximal section of the dissection flap. In the others in the center of the distal section of the dissection flap. The fenestration in the dissection flap was made by a 10 millimeter by 40 millimeter Percutaneous Transluminal Angioplasty balloon (Abbott Vascular, California, USA) (Figure 1.).

## In-vitro circulatory system

A validated in-vitro circulatory system with physiological flow and pressure characteristics was used to mimic the human circulatory system.[10, 12, 13] The main components of this circulatory system are a pneumatically-driven pulsatile pump, a compliance chamber and the watertight synthetic box with the aortic dissection model (Figure 2). All components are connected by a silicone tubing system and water was used for circulating fluid with a small concentration of contrast agent (Ultravist, Bayer, Germany). During the experiments the pneumatically-driven pulsatile pump was set on the parameters presented in table 2. The synthetic box with the aortic dissection model was placed inside the CT gantry.

## Imaging and data processing

Computed tomography (Toshiba Aquilion One Genesis Edition™ Japan) was used for imaging making 1 millimeter slices. The lumen area of one slice proximal to the dissection was determined in each phase of the systolic and diastolic cardiac cycle, using Mass Research Software (Leiden University Medical Center) with manual contour segmentation (Figure 3).[14] Each phase was analyzed

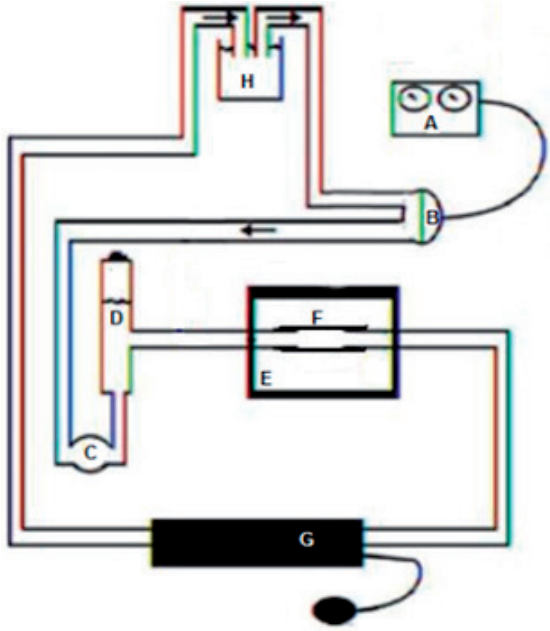


**Figure. 2.** Circulation set-up. A schematic representation of the circulation set-up, which consisted of an artificial heart driver (A), left ventricle (B), a ball valve (C), an air chamber (D), a watertight synthetic box (E), theaortic dissection model (see Fig. 2) (F), a blood pressure cuff (G), and an open reservoir (H).

and the phase with the largest lumen area was chosen for volume calculations of the false and true lumen using in-house developed software with manual contour segmentation.

Two CT-scans per model were made; one at baseline (without any fenestration) and one after fenestration of the dissection flap.

## RESULTS

The general flow characteristics of the in vitro circulation in the models are presented in Table 1. The models had a similar morphology at baseline but differed in lumen diameter and dissection width resulting in differences in True Lumen Volume (TLV) and False Lumen Volume (FLV) as presented in Table 2. Balloon fenestration of the dissection flap was performed in model 1, 3 and 5 proximally and in model 2, 4 and 6 distally.

### Proximal fenestration of the dissection flap

Performing a fenestration in the proximal section of the dissection flap resulted in FLV increase in models 3 and 5. However in model 1 it resulted in FLV decrease (Table 2.). The average false lumen volume change of minus 0.7% (SD 2.9%) was observed after proximal fenestration.

## Distal fenestration of the dissection flap

Performing a fenestration in the distal section of the dissection flap resulted in FLV decrease in all three models. The average false lumen volume change of minus 9.6% (SD 3.5%) was observed after fenestration (Table 2.).

False lumen reduction was obtained significantly in the distal fenestrated models compared to the proximal fenestrated models (9.6±3.5% vs. 0.7±2.9%, *p=0.03*)

**Table I.** In vitro circulatory system flow characteristics

| In vitro circulatory system flow characterictics | |
|---|---|
| Heart beat/min | 70 |
| Systolic pressure | 130-mm Hg |
| Diastolic pressure | 70-mm Hg |
| Mean stroke volume/beat | 40 mL |
| Output volume/min | 2800 mL |

**Table II.** True and false lumen outcomes by model

| Model | True lumen volume (TLV) (mL) | False lumen volume (FLV) (mL) | False lumen % of total lumen volume | False lumen change | *P* value |
|---|---|---|---|---|---|
| 1 | | | | | |
| Baseline | 9.75 | 6.25 | 39.0 | | |
| Proximal fenestration | 11.42 | 6.17 | 35.1 | | |
| | | | | -3.9% | |
| 3 | | | | | |
| Baseline | 10.76 | 4.42 | 29.1 | | |
| Proximal fenestration | 10.65 | 4.73 | 30.8 | | |
| | | | | 1.7% | |
| 5 | | | | | |
| Baseline | 18.52 | 15.36 | 45.3 | | |
| Proximal fenestration | 17.21 | 14.32 | 45.4 | | |
| | | | | 0.1% | |
| Model | | | | | |
| 2 | | | | | |
| Baseline | 10.25 | 8.88 | 46.4 | | |
| Distal fenestration | 11.82 | 8.13 | 40.7 | | 0.03 |
| | | | | -5.7% | |
| 4 | | | | | |
| Baseline | 9.18 | 5.16 | 36.0 | | |
| Proximal fenestration | 11.37 | 3.91 | 25.6 | | |
| | | | | -104% | |
| 6 | | | | | |
| Baseline | 6.01 | 5.97 | 49.8 | | |
| Proximal fenestration | 7.28 | 4.3 | 37.1 | | |
| | | | | -12.7% | |

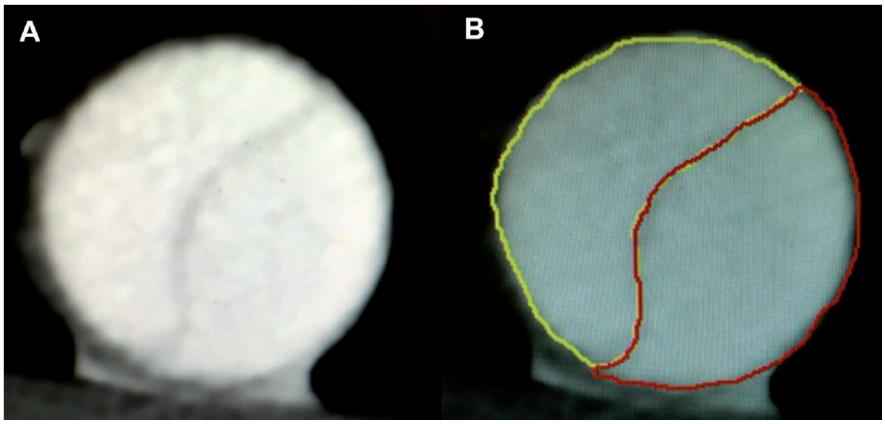


**Figure. 3.** (A) and (B). Transverse CT image of model 2 at the beginning of the dissection with manually marked contours (B) of the false lumen (red) and true lumen (yellow).

## DISCUSSION

Endovascular aortic fenestration quickly reduces the high pressure in the false lumen by communicating the false with the true lumen.[15] It remains unclear where the optimal location of these fenestrations should be chosen. We hypothesized that distal fenestration of the false lumen will result in the largest false lumen reduction and thereby more adequate depressurisation of the false lumen. An ex-vivo study was performed with porcine aortas with a surgically-constructed false lumen to study this hypothesis.

In only one of the three aortic models with a balloon fenestration in the proximal part of the dissection flap FLV reduction was observed. In the others two aortic models a slight FLV increase was observed. These results are in contrast with the FLV's of the models where a balloon fenestration in the distal section of the dissection flap was performed. All three dissection models with a balloon fenestration in the distal section of the dissection flap showed a FLV decrease. The observations of this ex-vivo study are that performing a distal fenestration in the dissection flap result in significant ($p=0.03$) FLV decrease compared to performing a proximal fenestration.

Ex-vivo models are useful to study hemodynamic changes in aortic pathologies. Factors in this complex circulation system can be isolated and analyzed. Previous ex-vivo studies used synthetic polymer or silicon tubing for simulating aortic dissection in contrast to the used porcine aorta in our model. [16, 17] The morphology of the surgically created false lumen is comparable to a human aortic dissection as showed in previous publication.[18] Additionally we used CTA for imaging and volume measurements, this imaging modality is not previously described in in-vitro studies. [16-18] [19] Although volume of the false lumen and pressure in the false lumen are strongly correlated a drawback might be the fact that measurements of the pressure gradients were not performed. To study the changes of the pressure gradient in the false lumen invasive pressure measurement should be performed. In pilot experiments we found out that pressure measurements of the false

lumen by a cannula or pressure wire were highly influenced by the exact position of the cannula or pressure wire in the false lumen. During cardiac cycle the position of the tip of the cannula changed all the time and would not result in objective pressure measurements of the false lumen.

Translation of the results from the ex-vivo model to a physiological in-vitro situation is, of course, limited. The presented ex-vivo model has limitations. The circulatory medium was water instead of blood, which is not a thrombotic medium. Use of a thrombotic medium results in spontaneous thrombosis that could either block the tubing system, false lumen or disturb the function of the pulsatile pump.[18] The porcine aortas were prepared, frozen, and thawed after 1 day, which might have altered the elastic properties of the arterial wall. Thirdly the aortic model was not surrounded by connective tissue, which will influence the compliance of the true and false lumen.

Endovascular treatment of aortic dissection consists usually of implantation of thoracic tubular stent-grafts to cover the proximal entry tear and redirect flow into the true lumen.[1] Aortic fenestration is still in use in malperfusion syndromes and in cases not suitable for proximal aortic tear coverage. [3,5,8] The advantages of endovascular aortic fenestration are directly relieving organ or limb ischemia in a faster way than by aortic graft replacement. Although aortic fenestration is rarely used it should be in one's endovascular therapeutic arsenal for treating aortic dissections.

Further ex-vivo experiments are required to obtain more insight between different types of dissections with different morphology and vascular wall characteristics. But also the role of fenestrations by branch vessels originating from the false lumen could be researched.

In conclusion, in this ex-vivo study, we showed that performing a fenestration in the distal part of the false lumen in an aortic dissection will result in the largest false lumen reduction. This observation might contribute in case endovascular fenestration must be performed.

## Acknowledgements

The authors wish to express their gratitude to Joost Roelofs for his invaluable assistance during the Computed Tomography experiments.

## REFERENCE LIST


(1) Scott AJ, Bicknell CD. Contemporary Management of Acute Type B Dissection. Eur J Vasc Endovasc Surg 2016 Mar;51(3):452-9.

(2) Wolfschmidt F, Hassold N, Goltz JP, Leyh R, Bley TA, Kickuth R. Aortic Dissection: Accurate Subintimal Flap Fenestration by Using a Reentry Catheter with Fluoroscopic Guidance-Initial Single-Institution Experience. Radiology 2015 Sep;276(3):862-72.

(3) Vendrell A, Frandon J, Rodiere M, Chavanon O, Baguet JP, Bricault I, et al. Aortic dissection with acute malperfusion syndrome: Endovascular fenestration via the funnel technique. J Thorac Cardiovasc Surg 2015 Jul;150(1):108-15.

(4) Panneton JM, Teh SH, Cherry KJ, Jr., Hofer JM, Gloviczki P, Andrews JC, et al. Aortic fenestration for acute or chronic aortic dissection: an uncommon but effective procedure. J Vasc Surg 2000 Oct;32(4):711-21.

(5) Pradhan S, Elefteriades JA, Sumpio BE. Utility of the aortic fenestration technique in the management of acute aortic dissections. Ann Thorac Cardiovasc Surg 2007 Oct;13(5):296-300.

(6) Iyer V, Harlock J. A new and forgotten indication for aortic fenestration. J Endovasc Ther 2011 Apr;18(2):261-2.

(7) Nienaber CA, Eagle KA. Aortic dissection: new frontiers in diagnosis and management: Part II: therapeutic management and follow-up. Circulation 2003 Aug 12;108(6):772-8.

(8) Midulla M, Renaud A, Martinelli T, Koussa M, Mounier-Vehier C, Prat A, et al. Endovascular fenestration in aortic dissection with acute malperfusion syndrome: immediate and late follow-up. J Thorac Cardiovasc Surg 2011 Jul;142(1):66-72.

(9) Pradhan S, Elefteriades JA, Sumpio BE. Utility of the aortic fenestration technique in the management of acute aortic dissections. Ann Thorac Cardiovasc Surg 2007 Oct;13(5):296-300.

(10) Veger HT, Westenberg JJ, Visser MJ. The role of branch vessels in aortic type B dissection: an in vitro study. Eur J Vasc Endovasc Surg 2015 Apr;49(4):375-81.

(11) Qing KX, Chan YC, Lau SF, Yiu WK, Ting AC, Cheng SW. Ex-vivo haemodynamic models for the study of Stanford type B aortic dissection in isolated porcine aorta. Eur J Vasc Endovasc Surg 2012 Oct;44(4):399-405.

(12) Bosman WM, Vlot J, van der Steenhoven TJ, van den Berg O, Hamming JF, de Vries AC, et al. Aortic Customize: an in vivo feasibility study of a percutaneous technique for the repair of aortic aneurysms using injectable elastomer. Eur J Vasc Endovasc Surg 2010 Jul;40(1):65-70.

(13) Hinnen JW, Rixen DJ, Koning OH, Van Bockel HJ, Hamming JF. Aneurysm sac pressure monitoring: does the direction of pressure measurement matter in fibrinous thrombus? J Vasc Surg 2007 Apr;45(4):812-6.

(14) van der Geest RJ, Reiber JH. Quantification in cardiac MRI. J Magn Reson Imaging 1999 Nov;10(5):602-8.

(15) Swee W, Dake MD. Endovascular management of thoracic dissections. Circulation 2008 Mar 18;117(11):1460-73.

(16) Chung JW, Elkins C, Sakai T, Kato N, Vestring T, Semba CP, et al. True-lumen collapse in aortic dissection: part II. Evaluation of treatment methods in phantoms with pulsatile flow. Radiology 2000 Jan;214(1):99-106.

(17) Tsai TT, Schlicht MS, Khanafer K, Bull JL, Valassis DT, Williams DM, et al. Tear size and location impacts false lumen pressure in an ex vivo model of chronic type B aortic dissection. J Vasc Surg 2008 Apr;47(4):844-51.

(18) Qing KX, Chan YC, Lau SF, Yiu WK, Ting AC, Cheng SW. Ex-vivo haemodynamic models for the study of Stanford type B aortic dissection in isolated porcine aorta. Eur J Vasc Endovasc Surg 2012 Oct;44(4):399-405.

(19) Faure EM, Canaud L, Cathala P, Serres I, Marty-Ane C, Alric P. Human ex-vivo model of Stanford type B aortic dissection. J Vasc Surg 2014 Sep;60(3):767-75.

# 6

# General Discussion

The studies presented in this thesis provide novel insight in mechanistic aspects of the dissection process. Although it is clear that treatment of cTBAD with TEVAR has resulted in improved outcomes optimal management of uTBAD at presentation remains an issue of much debate. First, the in hospital mortality of this group patients treated medically is around 12 % and secondly without early intervention there is a 20% long term risk of significant aortic aneurysm formation.[1] The current treatment paradigm of TEVAR in uTBAD when complications develop is based on the unfavorable risk-to-benefit ratio previously associated with TEVAR. As the discussion continues whether to treat acute uTBAD by early TEVAR it is of great importance to identify patients at risk of developing cTBAD and at the same assesment of risk factors leading to complications due to TEVAR should be defined and reduced.

## uTBAD CONVERTING TO cTBAD

Most previous studies have looked at clinical parameters or CTA based anatomic characteristics that may predict an adverse outcome. Some of these predictors can be used in the clinical setting to advocate early intervention in uTBAD. However there is little knowledge on basic mechanistic pathofysiologic processes that define the dissection process and in particular false lumen behaviour. Therefore we created a porcine model to experimentally examine some anatomic and haemodynamic elements and used clinical imaging studies to delineate the dissection process.

Incomplete thrombosis or patent false lumen portends a poor outcome.[2 3 4] The occurrence of thrombosis in the false lumen depends on coagulability, endothelial injury/dysfunction and blood flow. The blood flow in the false lumen is highly variable due to morphological differences between various types of dissections. [5]

It is conceivable that patent branch vessels originating from the false lumen in TBAD may contribute to persistent blood flow and patent false lumen, and thus to prognosis. Our in-vitro study showed that outflow through a branch vessel originating from the false lumen in TBAD results in expansion of cross-sectional false lumen area. False lumen expansion might result in higher stress in the aortic wall, increasing the risk of dilatation which contributes to the conversion of uTBAD into cTBAD. Besides the limitations inherent to replicating in vivo conditions as discussed later in this section the model represents an TBAD with an intact dissection flap with no distal tear or partial thrombosis occluding distal tears, impending outflow resulting in a blind sac from where a single branch vessel originates.

The majority of experimental flow studies in the field of aortic diseases are based on rigid wall models, under the assumption that the effect of wall elasticity on the quantitative results is rather limited for the haemodynamic parameters studied. Although it is known that aortic wall elasticity is variable and often altered in aortic dissections. [6]

We showed in a porcine aortic dissection model that aortic wall elasticity is an important parameter altering the false lumen. An aortic wall with reduced elasticity results in an increased

false lumen diameter in the mid and distal part of the false lumen. These results support the evidence that wall elasticity is clearly altering intraluminal haemodynamics compared to a rigid-wall simulation and should be taken into account when assessing and studying aortic dissections. This highlights the potential of new non-invasive imaging techniques that can give us the hemodynamic information compared to conventional imaging modalities.

The gold standard for imaging TBAD is Computed Tomography Angiography (CTA). [7]

However, because of the static aspect of CTA images, interpretation of the volume and flow changes in the true and false lumen during cardiac cycle is not possible. There are no clinical hemodynamic studies that help to predict the clinical behavior of acute TBAD. Hemodynamic parameters such as flow pattern, volume and velocity have a role in false lumen expansion. [8 9] 4D flow MRI can accurately visualize and quantify the functional flow and access hemodynamic information such as Wall Shear Stress. In arterial blood flow, the WSS expresses the viscous force per unit area applied by the fluid on the wall in a direction at the local interface. [10]

Earlier research on aortic dissection by 4D flow MRI was performed using silicon models mimicking chronic TBAD and resulted in hemodynamic insights. We focused on studying hemodynamics of the false lumen in acute TBAD simulated by a porcine aorta model. A significant increase in FLV, mean WSS and peak WSS was observed when heart rate raised from 60 to 80 baets per minute (bpm). These results support the recommendations of goal-directed therapy to establish and control a heart rate of less than 60 bpm in the 2010 ACCF/AHA/AATS/ACR/ASA/SCA/SCAI/SIR/STS/SVM Guidelines for the Diagnosis and Management of Patients With Thoracic Aortic Disease. [11]

When the HR raised from 80 to 100 bpm, no significant increase in FLV was observed but increase of mean and peak WSS were measured. This finding indicates that a stable FLV does not exclude an increase in mean and peak WSS. It illustrates the added value of 4D MRI, in gaining additional hemodynamic information compared to conventional imaging modalities. In uTBAD 4D flow MRI could be implemented as additional imaging to understand the WSS at presentation but also during OMT. It might be of relevance in the future as this knowledge can suggest more aggressive blood pressure lowering therapy and better heart rate control as well as to select those who will benefit from early intervention.

## INTERVENTION RISK

Retrograde dissection, spinal cord ischemia and paraplegia are known complications after TEVAR. Retrograde dissection is the most feared complication of TEVAR and it is of great importance to prevent retrograde dissection. The stress yielded by the endograft seems to play a predominant role in its occurrence. The currently available stentgrafts have been designed for thoracic atherosclerotic aneurysms, a different disease where strong radial force for adequat sealing is needed. Gently transferred forces (radial and "spring-back" force) of the stentgraft on the fragile inner

wall at the proximal landing zone in aorta dissection are crucial to prevent intimal damage and thereby the occurance of a new tear. As the spring-back force is an important factor in the stent graft-induced injury as the more the endograft is bent, the higher the stress might be. Also is there increased stress at the end closer to the curving point of the endograft than at the other end. A dissection-specific stentgraft calls for lower radial force and higher flexibility (reduced "spring-back" force). The diameter of the distal true lumen would be added into the preoperative sizing, and a tapered device might be conducive if the distal true lumen is far smaller than the proximal landing zone. Research on the currently available stentgrafts and the radial and "spring-back" force will show the stentgraft with the best characteristics. Another aspect of TEVAR is the layer of fabric that covers the intercostal arteries and can result in postprocedural new-onset paraplegia due to ischemic spinal cord injury. The dissection-specific stentgraft could be a hybrid design of proximal covered and distale bare stents.

In cTBAD malperfusion is caused by dynamic or static obstruction. Endovascular aortic fenestration quickly reduces the high pressure in the false lumen by communicating the false with the true lumen directly relieving organ or limb ischemia in a faster way than by aortic graft replacement. [12 13] It is useful in malperfusion syndromes and in cases not suitable for proximal aortic tear coverage. [12 13] A recent study shows that cTBAD complicated by malperfusion treated with endovascular fenestration/bare metal stenting has excellent short- and longterm outcomes.[14] It remains unclear where the optimal location of these fenestrations should be chosen. Two different fenestrations strategies in a validated ex-vivo porcine aorta dissection model in a pulsatile flow-model were studied. The observations were that performing a distal fenestration in the dissection flap resulted in significant false lumen volume decrease compared to performing a proximal fenestration. A more distal location of the fenestration in the false lumen lead to better equilibration of pressures and false lumen reduction. Endovascular fenestration/stenting is an effective tool to treat malperfusion (dynamic and static) in acute TBAD and is a valuable adjunct to both medical and surgical therapy (TEVAR and open repair).[14]

Due to limitations inherent to replicating in vivo conditions preclinical testing has a limited ability in reproducing clinical settings. Therefore, the limitations of the pulsatile flow model need to be addressed and suggestions for improvement are made. Water was used as a circulatory medium instead of blood, which has a different viscosity and is not a thrombotic medium. Spontaneous thrombosis could either block the tubing system or disturb the function of the pulsatile pump. The use of anticoagulation in the circulatory system might prevent this. The option of adjusting the viscosity of the circulatory fluid in the flow model would result in a more realistic simulation of the human circulatory system. Secondly the applied pulsatile flow was not equal to human aortic flow. Adding the aortic valve and arch to the porcine dissection model would have made it more representative. Thirdly the aortic model was submerged in water without support, which is not representative for the connective tissue normally surrounding the aorta. Beside the previously mentioned adjustments one could replace water for silicon with the same properties as human peri aortic connective tissue in future experiments to represent reality.

In conclusion, the studies described in this thesis used a created porcine TBAD model under pulsatile conditions to sort out the effects of biomechanical parameters on the false lumen in TBAD. For many decades fenestration of the false lumen is performed to achieve a quickly decrease of the pressure gradient of the false lumen. Untill our research it remained unclear where the optimal location of these fenestrations should be chosen. We showed in our model that distal fenestration of the false lumen in aortic dissection will result in the largest false lumen reduction.

We proved in our model that outflow through branch vessels of the false lumen, aortic wall compliance and hemodynamics have a major impact on the false lumen in uTBAD. The static aspect of CTA images makes it unpossible to be well informed on these biomechanical parameters. Advancement of non-invasive diagnostic imaging as 4D MRI should be further studied in the clinical setting as an alternative to the static imaging technique in current practice. This may help to better delineate risk factors that propagate a more complicated dissection course and determine which patients should undergo TEVAR in the early stages of uTBAD.

For our research group, the studies presented in this thesis form a foundation to formulate novel clinically driven questions related to TBAD. Continued research by our group will focus on the additional value of 4D MRI in acute uTBAD in clinical setting.

## REFERENCE LIST


(1.) Durham CA, Cambria RP, Wang LJ et al. The natural history of medically managed acute type B aortic dissection. J Vasc Surg 2015;61:1192-9.

(2.) Tsai TT, Evangelista A, Nienaber CA, et al. Partial thrombosis of the false lumen in patients with acute type B aortic dissection. N Engl J Med 2007;357:349–59.

(3.) Evangelista A, Salas A, Ribera A, Ferreira-Gonzalez I, et al. Long-term outcome of aortic dissection with patent false lumen: predictive role of entry tear size and location. Circulation 2012 Jun 26;125(25):3133-41.

(4.) Tanaka A, Sakakibara M, Ishii H, Hayashida R, et al. Influence of the false lumen status on short- and long-term clinical outcomes in patients with acute type B aortic dissection. J Vasc Surg 2013 Oct 16

(5.) Karmonik C, Bismuth J, Redel T, Anaya-Ayala JE, et al. Impact of tear location on hemodynamics in a type B aortic dissection investigated with computational fluid dynamics. Conf Proc IEEE Eng Med Biol Soc 2010;2010:3138-41.

(6.) Wu D, Shen YH, Russell L, Coselli JS, Lemaire SA. Molecular mechanisms of thoracic aortic dissection. J Surg Res. 2013;184(2):907-24.

(7.) Khayat M, Cooper KJ, Khaja MS, Gandhi R, et al. Endovascular management of acute aortic dissection. Cardiovasc Diagn Ther. 2018;8(Suppl 1):S97-S107

(8.) Tse KM, Chiu P, Lee HP, Ho P. Investigation of hemodynamics in the development of dissecting aneurysm within patient-specific dissecting aneurismal aortas using computational fluid dynamics (CFD) simulations J Biomech, 44 (2011), pp. 827-836

(9.) Cheng, FP, Tan, CV, Riga CD, Bicknell, MS et al. Analysis of flow patterns in a patient-specific aortic dissection model J Biomech Eng. 2010;132(5):051007

(10.) Katritsis D, Kaiktsis L, Chaniotis A, Pantos J, et al. Wall shear stress: theoretical considerations and methods of measurement. Prog Cardiovasc Dis. 2007;49(5):307-29.

(11.) Hiratzka LF, Bakris GL, Beckman JA, et al. ACCF/AHA/AATS/ACR/ASA/SCA/SCAI/SIR/STS/SVM guidelines for the diagnosis and management of patients with Thoracic Aortic Disease: a report of the American College of Cardiology Foundation/American Heart Association Task Force on Practice Guidelines, American Association for Thoracic Surgery, American College of Radiology, American Stroke Association, Society of Cardiovascular Anesthesiologists, Society for Cardiovascular Angiography and Interventions, Society of Interventional Radiology, Society of Thoracic Surgeons, and Society for Vascular Medicine. Circulation. 2010;121(13):e266-369.

(12.) Midulla M, Renaud A, Martinelli T, Koussa M, et al. Endovascular fenestration in aortic dissection with acute malperfusion syndrome: immediate and late follow-up. J Thorac Cardiovasc Surg 2011 Jul;142(1):66-7

(13.) Vendrell A, Frandon J, Rodiere M, Chavanon O, et al. Aortic dissection with acute malperfusion syndrome: Endovascular fenestration via the funnel technique. J Thorac Cardiovasc Surg 2015 Jul;150(1):108-15.

(14.) Norton EL, Williams DM, Kim KM, Khaja MS, et al. Management of acute type B aortic dissection with malperfusion via endovascular fenestration/stenting. J Thorac Cardiovasc Surg 2020;160:1151-61

# 7

## Summary

## Samenvatting in het Nederlands

## SUMMARY

The first part (Chapter 2) of this dissertation gives an introduction to Type B Aortic Dissection (TBAD). This overview shows several prognostic predictors of dissection related events (dissection related death or need for intervention) after initial medical management in acute uncomplicated TBAD. Predictors of complications in acute uTBAD during admission are aortic diameter ≥40mm, a primary entry tear >10mm, primary entry tear located on the concavity (undersurface) of the distal aortic arch, a FL diameter > 22mm, a peak CRP level >96mg/L and patency of the false lumen (defined as the concurrent presence of both flow and thrombus)..

The blood flow in the false lumen is highly variable due to morphological differences between various types of dissections. It is conceivable that patent branch vessels originating from the false lumen in an aortic dissection type B may contribute to persistent blood flow and patent false lumen, and thus to prognosis. Therefore, an in-vitro study was performed with a surgically-constructed false lumen and an adjustable outflow branch (Chapter 3.). This in-vitro study show that different outflow from branch vessels originating from the false lumen in TBAD result in expansion of cross-sectional false lumen area. This might have important consequences for patients with uTBAD when patent branch vessel(s) originating from the false lumen and partial thrombosis (occluding distal tears) or no distal tear are present, as these patients might be more at risk for developing complicated TBAD.

Haemodynamics, dissection morphology and aortic wall elasticity have a major influence on the pressure in the false lumen. The influence of haemodynamics and dissection morphology have been investigated often in multiple in-vitro and ex-vivo studies in contrast to aortic wall elasticity. In Chapter 4 the influence of aortic wall elasticity on the diameter and pressure of the false lumen in aortic dissection is studied in-vitro. It shows that aortic wall elasticity is an important parameter altering the false lumen. This in-vitro study showed that an aortic wall with reduced elasticity results in an increased false lumen diameter in the mid and distal part of the false lumen. False lumen expansion might result in higher stress of the aortic wall and at the ending of the dissection.

More insight in the hemodynamic changes during cardiac cycle in the true and false lumen of uncomplicated TBAD might result in prediction of adverse outcomes. Four-Dimensional flow Magnetic Resonance Imaging (4D flow MRI) compared to CTA provides insight into hemodynamic dimensions such as Wall Shear Stress. In arterial blood flow, the WSS expresses the viscous force per unit area applied by the fluid on the wall in a direction at the local interface. In Chapter 5. our ex-vivo research illustrates that an increase in heart rate (HR) from 60 to 80 bpm resulted in a significantly increase of the False Lumen Volume (FLV) and Wall Shear Stress (WSS) of the false lumen. Hereby we confirm that strict HR control is of major importance and reduces the mean and peak WSS in uncomplicated TBAD.

The first line therapy in TBAD with malperfusion syndrome is coverage of the proximal entry tear by Thoracic Endo-Vascular Aortic Repair (TEVAR). When this method is unfeasible, endovascular aortic fenestration has been proposed as an alternative technique. Fenestration is a

minimally invasive alternative for the treatment of acute symptomatic aortic dissections because it may quickly decrease the pressure gradient of the false lumen. It remains unclear where the optimal location of these fenestrations should be chosen. In Chapter 6. the false lumen volume after different fenestration strategies was studied. This in-vitro study showed that distal fenestration of the false lumen in aortic dissection will result in the largest false lumen reduction.

## SAMENVATTING IN HET NEDERLANDS

De behandeling van Type B Aorta Dissectie (TBAD) is tot op heden onderwerp van discussie. TBAD kan worden onderverdeeld in ongecompliceerd en gecompliceerd.

Bij een gecompliceerde TBAD (cTBAD) kan er sprake zijn van ruptuur, verstoorde doorbloeding van zijtakken van de aorta, snelle verwijding van de aorta of aanhoudende pijnklachten ondanks medicatie. Bij een ongecompliceerde TBAD (uTBAD) zijn de eerder genoemde complicaties er niet. Een onderverdeling in uTBAD is acuut (0-2 weken), sub acuut (2-6 weken) en chronisch (>6 weken).

De standaard behandeling bij een acute uTBAD is medicamenteuze behandeling. Dit betreft opname op een verpleegafdeling waar vitale parameters (bloeddruk, hartslag, ademhalingsfrequentie etc) continu gemonitord en behandeld kunnen worden. De hoekstenen van de medicamenteuze behandeling zijn bloeddruk en hartslag verlaging en adequate pijnstilling. Acute uTBAD kan verslechteren in cTBAD bij ongeveer 20% van de patienten. Als er eenmaal complicaties (ruptuur, verstoorde doorbloeding van zijtakken van de aorta, snelle verwijding van de aorta of aanhoudende pijnklachten ondanks medicatie) optreden neemt de prognose af waarbij de kans om te komen te overlijden meer dan 50% is.

Het eerste deel (Chapter 2) van dit proefschrift is een introductie over TBAD. Hierin worden een aantal voorspellende waarden benoemd die een negatieve invloed kunnen hebben op een ongecompliceerd beloop van een uTBAD. Voorspellende waarden voor dissectie gerelateerde complicaties bij acute TBAD bij opname zijn een gestoorde nierfunctie (eGFR <60 ml/min) en een maximale aorta diameter ≥40mm. Voorspellende waarden voor dissectie gerelateerde complicaties bij acute TBAD tijdens opname zijn een C-Reactive Protein >96mg/L en een doorgankelijk vals lumen. De bloeddoorstroming in het valse lumen is erg afhankelijk van de vorm van de dissectie. Zijtakken die uit het valse lumen bij uTBAD komen, kunnen bijdragen aan het niet opstollen van het valse lumen en daardoor mogelijk invloed hebben op de prognose.

De auteurs creëerden een aorta dissectie model door in een varkens aorta een kunstmatige dissectie te maken in de vaatwand. Het aorta dissectie model werd in een reeds gevalideerd circulatie systeem geplaatst. In dit aorta dissectie model werd de invloed van zijtakken die uit het valse lumen komen onderzocht (Chapter 3). Dit onderzoek toonde dat zijtakken resulteerden in een diameter toename van het valse lumen. Deze bevinding kan van waarde zijn voor patiënten met een uTBAD met zijtakken die uit het valse lumen komen, omdat deze groep mogelijk meer risico loopt op het ontwikkelen van een cTBAD.

Hemodynamiek, de vorm van de dissectie en wandelasticiteit van de aorta, hebben een belangrijke invloed op de druk in het valse lumen. De hemodynamiek en de vorm van de dissectie zijn in verschillende onderzoeken reeds bestudeerd dit is echter niet het geval voor de wand elasticiteit van de aorta. In Chapter 4 wordt de invloed van de wandelasticiteit van de aorta op de diameter en druk in het valse lumen bestudeerd. Dit onderzoek laat zien dat afname van de wandelasticiteit van de aorta resulteert in een diameter toename van het valse lumen in het middelste en uiteinde

van het valse lumen. Deze uitzetting van het valse lumen zou kunnen resulteren in een toename van de wandspanning ter plaatse.

Gedurende de hartslag zijn er hemodynamische veranderingen in het ware en valse lumen. Door dit beter inzichtelijk te krijgen, zou dit wellicht van waarde kunnen zijn in het voorspellen van complicaties bij uTBAD. Four-Dimensional flow Magnetic Resonance Imaging (4D flow MRI) geeft in vergelijking met Computed Tomography Angiography (CTA) wel informatie over de hemodynamiek, maar ook over de wandspanning (Wall Shear Stress – WSS). In Chapter 5 toont het onderzoek dat een toename van de hartslag van 60 naar 80 slagen per minuut resulteerde in een toename van het valse lumen én een toename van de wandspanning. Dit bevestigt dat het verlagen van de hartslag van cruciaal belang is omdat het de wandspanning (WSS) verlaagd.

De eerste keuze van behandeling in cTBAD, waarbij er een verstoorde doorbloeding van zijtakken is een Thoracic Endo-Vascular Aortic Repair (TEVAR). Als dit niet mogelijk is is endovasculaire aorta fenestratie een alternatieve techniek om cTBAD te behandelen. Fenestratie van het valse lumen resulteert in een snelle druk afname van het valse lumen.

Het is echter niet duidelijk op welke plaats de fenestratie in het valse lumen gemaakt moet worden voor het beste effect. In Chapter 6 worden verschillende fenestratie strategieën bestudeerd. Deze studie toont aan dat het maken van een fenestratie in het valse lumen aan het uiteinde van de dissectie resulteert in de grootste reductie van het valse lumen.

# 8

**List of Abbreviations**
**Acknowledgments (Dankwoord)**
**List of publications**
**Curriculum Vitae**

## LIST OF ABBREVIATIONS

| | |
|---|---|
| AD | Aortic Dissection |
| ABAD | Acute type B Aortic Dissection |
| CBAD | Chronic type B Aortic Dissection |
| CTA | Computed Tomography Angiography |
| FLV | False Lumen Volume |
| HR | Heart Rate |
| MRA | Magnetic Resonance Angiography |
| TAAD | Type A Aortic Dissection |
| TBAD | Type B Aortic Dissection |
| uTBAD | uncomplicated Type B Aortic Dissection |
| cTBAD | complicated Type B Aortic Dissection |
| TEVAR | Thoracic aortic endovascular repair |
| TLV | True Lumen Volume |
| TTE | TransThoracic Echocardiography |
| WSS | Wall Shear Stress |
| 4D MRI | Four-Dimensional flow Magnetic Resonance Imaging |

## ACKNOWLEDGMENTS (DANKWOORD)

De totstandkoming van dit proefschrift had niet kunnen plaats vinden zonder de hieronder genoemde collega's, vrienden en familie.

Allereerst wil ik Michel bedanken voor de begeleiding in het begin van mijn onderzoeks carrière en de vele (theoretische) brainstorm sessies. Helaas zijn onze wegen gescheiden geraakt in de loop van het onderzoek.

Beste Jos, vanaf het begin was jij meteen enthousiast en erg meedenkend om de flow model opstelling in de MRI te krijgen. Vele scan uren hebben we in de MRI doorgebracht wat uiteindelijk tot dit mooie resultaat heeft geleid. Je passie en toewijding voor de cardiovasculaire MRI zijn indrukwekkend.

Beste Erik, als student ben je halverwege het onderzoek aan boord gekomen. Je inzet en doorzettingsvermogen heb ik altijd erg gewaardeerd. Wat is het leuk om nu samen in de kliniek te werken.

Beste Randolph en Jan, wat is het geweldig om sinds 2016 onderdeel van het vaatchirurgische team in het Haga Ziekenhuis te zijn.

Beste Jaap, dank voor de begeleiding van mijn promotie traject waardoor dit proefschrift nu voor ons ligt.

Lieve pa en mam, ik ben jullie dankbaar voor de mogelijkheden die jullie mij hebben gegeven om mezelf te ontwikkelen. Jullie hebben voor mij de basis gelegd voor waar ik nu sta.

Mijn paranimfen Dimitri en Erik wil ik bedanken voor hun steun en hulp in de organisatie rondom de promotie.

Lieve Dik en Linda bedankt voor jullie enthousiasme en advies.

Lieve Ophélie en Taeke, jullie zijn altijd mijn drijfveer geweest. Jullie zijn mijn grote trots!

Allerliefste Melissa, jouw onvoorwaardelijke liefde, steun, begrip en geduld hebben de voltooiing van dit proefschrift mede mogelijk gemaakt. Het is fantastisch om met jou samen door het leven te gaan! Samen met onze geweldige kinderen kunnen we alles aan!

# LIST OF PUBLICATIONS

## In peer-reviewed journals

### This thesis

1. **H.T.C. Veger**, J. Hamming, M.J.T. Visser; *Understanding acute aortic type B dissection; are there new horizons in patient selection?* Reviews in Vascular Medicine 2013.
2. **H.T.C. Veger**, J.J.M. Westenberg, M.J.T. Visser; *The role of branch vessels in aortic type B dissection. An In-vitro study.* Eur J Vasc Endovasc Surg 2015.
3. **H.T.C. Veger**, E.H. Pasveer, J.J.M. Westenberg, J.J. Wever, R.G. Statius van Eps; *The influence of aortic wall compliance on false lumen expansion in aortic dissection. An in-vitro study.* Vascular and Endovascular Surgery 2020.
4. **H.T.C. Veger**, E.H. Pasveer, J.J.M. Westenberg, J.J. Wever, R.G. Statius van Eps; *Wall shear stress assessment of the false lumen in acute type B aortic dissection visualized by four-dimensional flow magnetic resonance imaging (4D flow MRI). An ex-vivo study.* Vascular and Endovascular Surgery 2021.
5. **H.T.C. Veger**, E.H. Pasveer, M.J.T. Visser; *Where to fenestrate in type B aortic dissection? An ex-vivo study.* Ann Vasc Surg 2017.

### Others

1. M.A. van Dam, M. Strietman, R.G.S. van Eps, , J.J. Wever, **H.T.C. Veger**; *Clinical relevance of Closed-Incision Negative Pressure Therapy (ciNPT) for groin incisions in vascular surgery. A prospective study with retrospective comparison of a standard-care group.* Ann Vasc Surg 2022.
2. W. Stomp W, J.E. Dierikx, J.J. Wever, L.C. van Dijk, R.G.S. van Eps, **H.T.C. Veger**, H. van Overhagen; *Percutaneous EVAR for ruptured abdominal aortic aneurysms using the Cordis INCRAFT endograft.* Ann Vasc Surg 2021.
3. L. Konijn, R. Tackx, W. Mali, **H.T.C. Veger**, H. van Overhagen; *Different lower extremity arterial calcification patterns in patients with chronic limb-threatening ischemia compared with asymptomatic controls.* J Pers Med. 2021.
4. E. Knöps, J. van Schaik, K.E.A. van der Bogt, **H.T.C. Veger**, H. Putter, E.J. Waasdorp, J.R. van der Vorst; *Stent graft sizing for endovascular abdominal aneurysm repair using open source image processing software. Ann Vasc Surg 2021.*
5. S.I. Willemsen, M.G. ten Berge, R.G.S. van Eps, **H.T.C. Veger**, H. van Overhagen, L.C. van Dijk, H. Putter, J. J. Wever; *Nationwide study to predict colonic ischemia after abdominal aortic aneurysm repair in The Netherlands.* Ann Vasc Surg 2020.
6. L.C.D. Konijn, T. Wakkie, M.I. Spreen, P.A. de Jong, L.C. van Dijk, J.J. Wever, **H.T.C. Veger**, R.G.S. Statius van Eps, W.P. Mali, H. van Overhagen; *10-Year paclitaxel dose-related outcomes of drug-eluting stents treated below the knee in patients with chronic limb-threatening ischemia (The PADI Trial).* Cardiovasc Intervent Radiol. 2020.

7. L.C.D. Konijn, H. van Overhagen, R. Takx, P.A. de Jong, **H.T.C. Veger**, W.P. Mali; *CT calcification patterns of peripheral arteries in patients without known peripheral arterial disease.* Eur J Radiol. 2020.
8. **H.T.C. Veger**, R.G.S. van Eps, J.J. Wever, H. van Overhagen, L.C. van Dijk; *Chimney Technique to Preserve Visceral flow in a Coral Reef Aorta.* Ann Vasc Surg. 2020.
9. T. Wakkie, L. Konijn, N.P.C. van Herpen, M.F.H. Maessen, M.I. Spreen, J.J. Wever, R.G. Statius van Eps, **H.T.C. Veger**, LC van Dijk, W.P. Mali, H. van Overhagen; *Cost-effectiveness of drug-eluting stents for infrapopliteal lesions in patients with critical limb ischemia: the PADI Trial.* Cardiovasc Intervent Radiol. 2020.
10. Q. Dang, R.G. Statius van Eps, J.J. Wever, **H.T.C. Veger**; *Nationwide study of the treatment of mycotic abdominal aortic aneurysms comparing open and endovascular repair in The Netherlands*. J Vasc Surg. 2020.
11. T.H.N. Ngo, B. Nemeth, **H.T.C. Veger**, J.J. Wever, A.T.A. Mairuhu, K. de Laat, R.G. Statius van Eps; *Clinical outcomes of post-carotid endarterectomy hypertension.* J Vasc Surg. 2019.
12. E. Pasveer, R.G.S. van Eps, J.J. Wever, H. van Overhagen, L.C. van Dijk, **H.T.C. Veger**; *Endovascular revascularisation of a chronic occluded aortobifemoral bypass*. Ann Vasc Surg. 2019.
13. R.G. Statius van Eps, B. Nemeth, R. Mairuhu, J.J. Wever, **H.T.C. Veger**, H. van Overhagen, L. van Dijk, B. Knippenberg; *Determinants of acute kidney injury and renal function decline after endovascular abdominal aortic aneurysm repair.* Eur J Vasc Endovasc Surg. 2017.
14. E.H. Pasveer, R.G. Statius van Eps, J.J Wever, **H.T.C. Veger**; *Multi-level mycotic aneurysms due to Salmonella infection: case report and review of the literature*. Ann Vasc Surg. 2017.
15. J. Brouwers, **H.T.C. Veger**, R. van Wissen, J. Rothmans, M.J.T. Visser; *Predictive value of intrarenal echo-Doppler by renal artery stenosis*. Vascular 2017
16. **H.T.C. Veger**, B. Borger van de Burg, M.J.T. Visser, P. Ph. Hedeman Joosten; *Popliteal artery injury after low-energy knee dislocation in the obese.* J Vasc Med Surg. 2015.
17. **H.T.C. Veger**, P. Ph. Hedeman Joosten, S.R. Thoma, M.J.T. Visser. *Infection of endovascular abdominal aortic aneurysm stent graft after urosepsis: case report and review of the literature*. Vascular 2013.

## CURRICULUM VITAE

Hugo Thomas Christian Veger was born on the 19th of August, 1982, in Dronten, The Netherlands. He attended high school Rembrandt College (atheneum), from which he graduated in 2000. Subsequently he started medical school at the University of Leiden and passed his Medical Degree (MD) in 2006. During his study and internships, he gained interest in surgery. He started as surgical resident (ANIOS) at the Department of Surgery in the Haga Hospital in The Hague. In 2008 he started his surgical residency in training at the Rijnland Hospital Leiderdorp under supervision of dr. S.A. da Costa and dr. A.M. Zeillemaker. In the beginning of his residency vascular surgery piqued his interest. The academical surgical residency in training (2010 – 2012) was done at the Leiden University Medical Center (LUMC) under supervision of prof. dr. J.F. Hamming. In 2013 he performed an endovasculair fellowship at the Ghent University Hospital (Belgium) under supervision of prof. dr. F. Vermassen. In 2014 he started a 2-year fellowship Vascular and Endovascular Surgery at the Zuyderland Medical Center in Heerlen. In 2015 he passed the Fellow of the European Board of Vascular Surgery (FEBVS) examination with honours. Since 2016 he is working as a consultant vascular surgeon in the Haga Hospital in The Hague. Hugo is married with Melissa, together they have two children; Ophélie (2014) and Taeke (2015).